6071

VISIBILITY LABORATORY
TECHNICAL REPORT 74-1

EXPERIMENTAL TVI SYSTEM REPORT

UNIVERSITY OF CALIFORNIA SAN DIEGO

SCRIPPS INSTITUTION OF OCEANOGRAPHY

VISIBILITY LABORATORY San Diego, California 92152

UNIVERSITY OF CALIFORNIA

BERKELEY • DAVIS • IRVINE • LOS ANGELES • RIVERSIDE • SAN DIEGO • SAN FRANCISCO

SANTA BARBARA • SANTA CRUZ

MARINE RESEARCH DIVISION

MAIL CODE A-031
LA JOLLA, CALIFORNIA 92093

October 18, 1989

Dr., Kenneth J. Voss
Department of Physics
University of Miami
PO Box 248046
Coral Gables, FL 33124

Subject: Experimental TVI System Report, Visibility Lab. Tech. Report 74-1

Dear Ken:

Enclosed for your retention is a copy of the subject report. The work was done in the early 1970's and the original version of the enclosed report was submitted in July and October of 1974 in two parts as summary reports on the design and on the test and evaluation effort. Because of a recurring interest in laser scanner systems, the reports have been reissued but combined as a single publication.

The TVI (Time Varying Intensity) system consists of a diver held underwater laser scanner that illuminates a scene or object of interest with a TV-like raster, and a shipboard receiver and display console that receives the light reflected from the scene and propagated to the receiver as modulated scattered light where it is decoded and displayed. The advantages of this system are: 1) the swimmer is unencumbered by umbilicals, 2) the laser illuminator provides extremely large depth of field, and 3) the use of image-encoded scattered light to transmit the scene information to the support vessel allowed object-to-receiver distances of 10 to over 20 attenuation lengths (i.e., r*c) in laboratory tank tests.

The equipment was designed for proof of concept tests and used technology which is now 16 or more years old. It performed well above our expectations and was capable of providing images with exquisite detail and clarity. Its application is probably for detail inspection of submerged objects under circumstances where, for whatever reason, normal U/W TV systems prove inadequate.

The current status of the equipment is as follows: The underwater laser scanner unit was destroyed in a catastrophic explosion of the silver-magnesium batteries while in their aluminum U/W canister. The U/W receiver components have been used on other programs. The control/display/storage console is still intact.

If you have questions regarding the TVI system or its possible applications we would be pleased discuss them with you.

Sincerely yours,

R.W. Austin
Director (retired)
Visibility Laboratory

Enclosure

Part II

Part II of this report will discuss test and evaluation of the experimental TVI system performed during July and August 1974. Tests include quantitative data on performance and evaluation includes underwater operation of the TVI system by divers.

Table of Figures

Tables

Table of Contents
Part I

University of California, San Diego
Scripps Institution of Oceanography
Visibility Laboratory
San Diego, California 92152

Experimental TVI System Report
Part I July 1974
Part II October 1974

Seibert Q. Duntley, Roswell W. Austin
Richard L. Ensminger, Theodore J. Petzold
Raymond C. Smith

Approval:

_____

S. Q. Duntley
Director Visibility Laboratory
and Principal Investigator

I. INTRODUCTION

The Visibility Laboratory has been conducting a program of research directed toward improving the capability of obtaining imagery in water. The overall program has included explorations of newly conceived unconventional concepts as well as performance analysis of more conventional systems and studies of ocean optical properties.

This report concerns one of the unconventional concepts. It is a system which produces high quality images through turbid waters by means of time-encoded reflected light which is transmitted by scattering. The initial embodiment of the concept consists of a compact, self-contained, battery operated laser scanning device capable of scanning an underwater scene with a laser beam in a manner similar to a television raster. Light reflected from any object in the scene varies in intensity according to the reflectance of the minute spot being illuminated. The time sequence of this light intensity is therefore encoded with scene reflectance information. This time varying intensity signal is transmitted through the water to a remote receiver by both scattered and unscattered light. The received signal is stored and/or displayed (like television) on a cathode ray tube using the precisely known time sequence of the underwater raster scan. The underwater laser scanner unit can be moved freely about the field of interest, unencumbered with entangling cables, and can send to a distant receiver real-time images for critical viewing by an operator monitoring the image display. The receiver may be separated from the object by many attenuation lengths of turbid water. This system, which utilizes long-range scattered light for transmitting the image from the object to the receiver, has been called imagery by means of time varying intensity (TVI).

This report presents the basic principles of remote imaging by means of time varying intensity (TVI), gives calculations and performance tests of system characteristics, describes rationale for the selected design, and outlines the development and testing of the first model of a useable TVI system. Later sections of this report will discuss system performance and limitations and also suggest recommendations for future development.

II. TIME VARYING INTENSITY (TVI) SYSTEM

A. Basic Principle

Fig. 1 shows a schematic diagram of the TVI system. The system consists of a self-contained underwater laser scanner unit, an underwater receiver unit, and a control/image storage/display unit. Detailed descriptions of these units are given below. Basically, the system transmits high quality images of the target scene by means of time encoded scattered light. An imaging sequence proceeds as follows.

The laser scanner is positioned within a few meters of the target and aimed at the desired portion of the scene to be imaged. Upon command, the laser scanner sends out a synchronizing pulse and then "paints" the scene with a television-like raster scan. The synchronizing pulse for the raster scan is transmitted through the water directly to a "sync" receiver at a remote location. Light from the raster scan of the laser is reflected from the target scene and is detected by a video receiver, also at

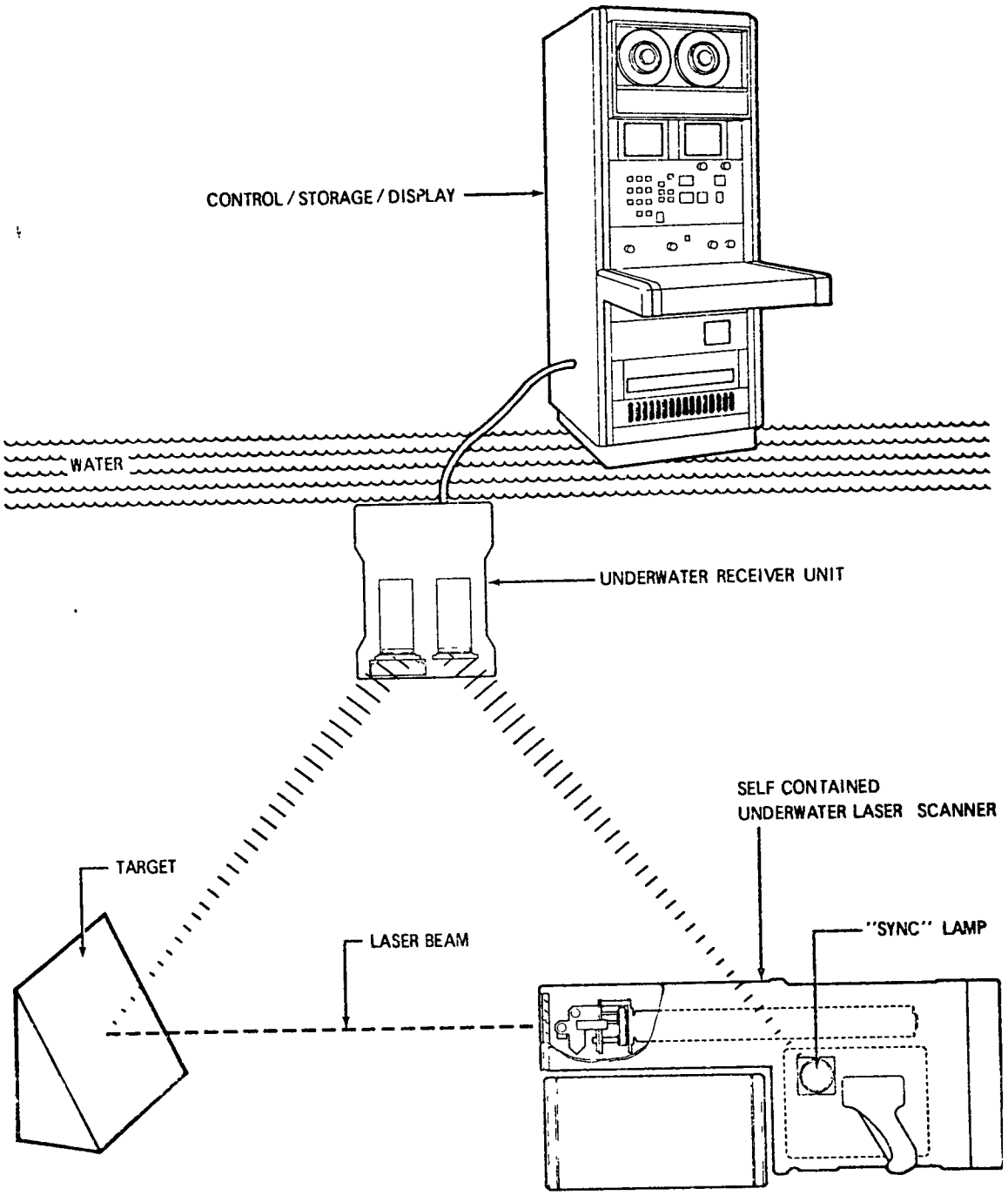

FIGURE 1. Schematic diagram of TVI experimental system showing the self-contained underwater laser scanner unit, the underwater receiver unit and the control/image storage/display unit.

the remote location. This reflected light from the scene travels through water at a speed of 735 feet per microsecond. It is time encoded with the reflectance properties of the scene, because each resolution element in the raster is sequentially illuminated. Thus, at any instant the flux detected by the distant receiver is proportional to the reflectance of a particular spot in the scene whose location within the raster is determined by the time of reception with respect to the synchronization pulse. The flux reflected from the target carries image information from the target to the receiver despite scattering along the intervening water path.

Detection by the TVI system is limited by the signal-to-noise ratio of the total light flux (sum of mono-path and multi-path signal components, see Appendix A) incident upon the receiver from the target. The field of view and the ultimate resolution of the system depend upon the number of resolution elements in the raster and the laser beam spot size. *The scanner uses a laser source, which has a very small beam divergence, making the depth of field very large compared to conventional camera systems. Freedom from a requirement to focus on the object of interest is believed to be an important advantage of TVI systems.*

Scattering between the laser scanner unit and the target causes a loss of image contrast because any light reaching the receiver which was backscattered by the water does not contain target information. However, the present TVI system has the important advantage that only one minute portion of the scene is illuminated at any one time. Thus, both backscatter and glow from the scene are greatly reduced in comparison with a conventional broad-beam lamp and camera system.

A TVI system using a laser scanner near the target to send a time varying intensity signal through the water to a remote receiver has important advantages over conventional imaging systems. (1) Its resolution capability can equal or exceed that of film cameras under comparable underwater conditions while retaining a real-time capability. (2) Compared to either photography or television the TVI system has a very large depth of field. Focusing is provided in the experimental model to "fine tune" the laser beam spot size for optimum resolution and has little effect on the useful depth of field. (3) TVI requires very much less total light in the water than does photography or television. (4) The light from the scanner can serve the diver somewhat like a flashlight; whatever it illuminates is seen by all observers watching the display(s) at the control panel. (5) A number of independent units can operate simultaneously without interference, because the laser light is nearly monochromatic and a number of frequencies are available. (6) Stereo viewing from a single unit may be accomplished with two wavelengths from the same laser by adding a small dichroic prism between two sets of scanners separated by a suitable baseline. Two receivers, properly filtered, would then be required as well as a stereo display.

B. System Components and Specifications

The TVI system described in this report was designed and fabricated to provide a working experimental model of a system capable of transmitting high quality images of an underwater scene by means of time-encoded reflected light. The experimental TVI system was designed with two, sometimes competing, objectives. First, the system was designed to have sufficient flexibility and signal analysis capability to enable a complete engineering analysis to be made and all of the basic TVI principles to be explored quantitatively. Second, it was designed so that the

feasibility of a TVI system could be tested and evaluated in a small, rugged, self-contained underwater unit capable of operation by a diver. The following sections describe the components and specifications of this first TVI system. Later sections of this report give the rationale for the choice of the components used, summarize the engineering calculations, and describe the laboratory tests of the completed experimental model.

1) Underwater Laser Scanner

A schematic diagram and photographs of the underwater laser scanner unit are shown in Figs. 2-5. This self-contained unit, operated by a diver, sends out a synchronizing pulse to begin an imaging sequence and then scans the target with a television-like raster scan using a laser beam. The unit contains a Helium-Neon (HeNe) laser, two galvanometer-type optical scanners, two Xenon flash lamps to emit omnidirectional synch pulses, power supplies, associated electronics and batteries. The unit is packaged for use by a diver at depths of 100 feet or less and is completely self-contained (i.e., *it does not require any form of umbilical connection to the receiver/display units*). The more important specifications of these components are as follows. Detailed specifications of the experimental TVI system's components are listed in Section II C.

Laser

A key component in the TVI system is the laser used as the light source for scanning the underwater target. A Coherent Radiation (Model No. 80-6) 6 milliwatt (CW, TEM_{00}, unpolarized) HeNe laser was selected for the experimental TVI system after tank tests and calculations showed that this small laser with proven ruggedness and reliability would suffice. Prime consideration was given to achieving adequate power (i.e., adequate image signal-to-noise ratio for useful target to receiver optical path lengths) while at the same time having sufficient portability and ruggedness for reliable field use. The compromises involved in this choice, along with possible alternative choices, are discussed in Appendix B. The 6 milliwatt red (632.8 nm) laser beam has a diameter of 0.7 mm (@ $1/e^2$ points) and a divergence of 1.15 milliradians. The laser and its DC power supply were selected to have less than 0.2% rms amplitude noise (1 Hz - 2 M Hz).

Galvanometer Scanners

The raster scan of the laser beam is accomplished by using two orthogonal mirrors mounted on low inertia, high speed, galvanometer drivers. The mirror sizes were chosen to accommodate the laser beam (diameter, plus divergence, plus scan angle) while at the same time obtaining an adequately fast scanning rate. Scanner mirror size increases the scanner inertia which in turn decreases the maximum possible scanning rate; thus beam spot size and scanning rate are inversely related. The optical scanners selected for the experimental TVI system (General Scanning Model G-0612), matched to the 0.7 mn laser beam diameter, have a calculated scanning frequency of at least 540 Hz (70% scan to wait time) when fitted with mirrors. Thus a 256 x 256 array of picture elements may be scanned in approximately one-half second. For example, if the laser beam is incident upon each resolution

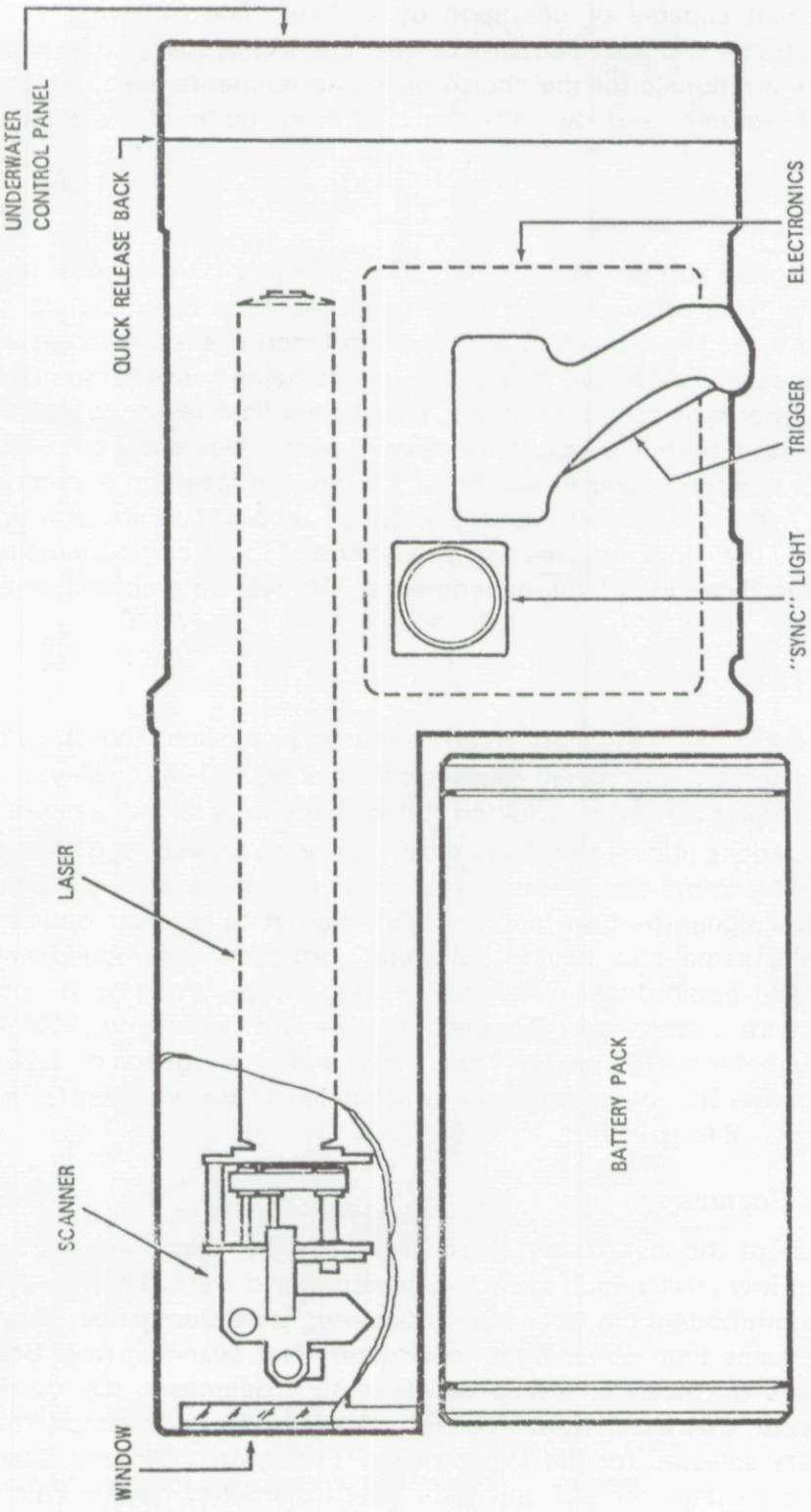

FIGURE 2. Schematic diagram of underwater laser scanner unit.

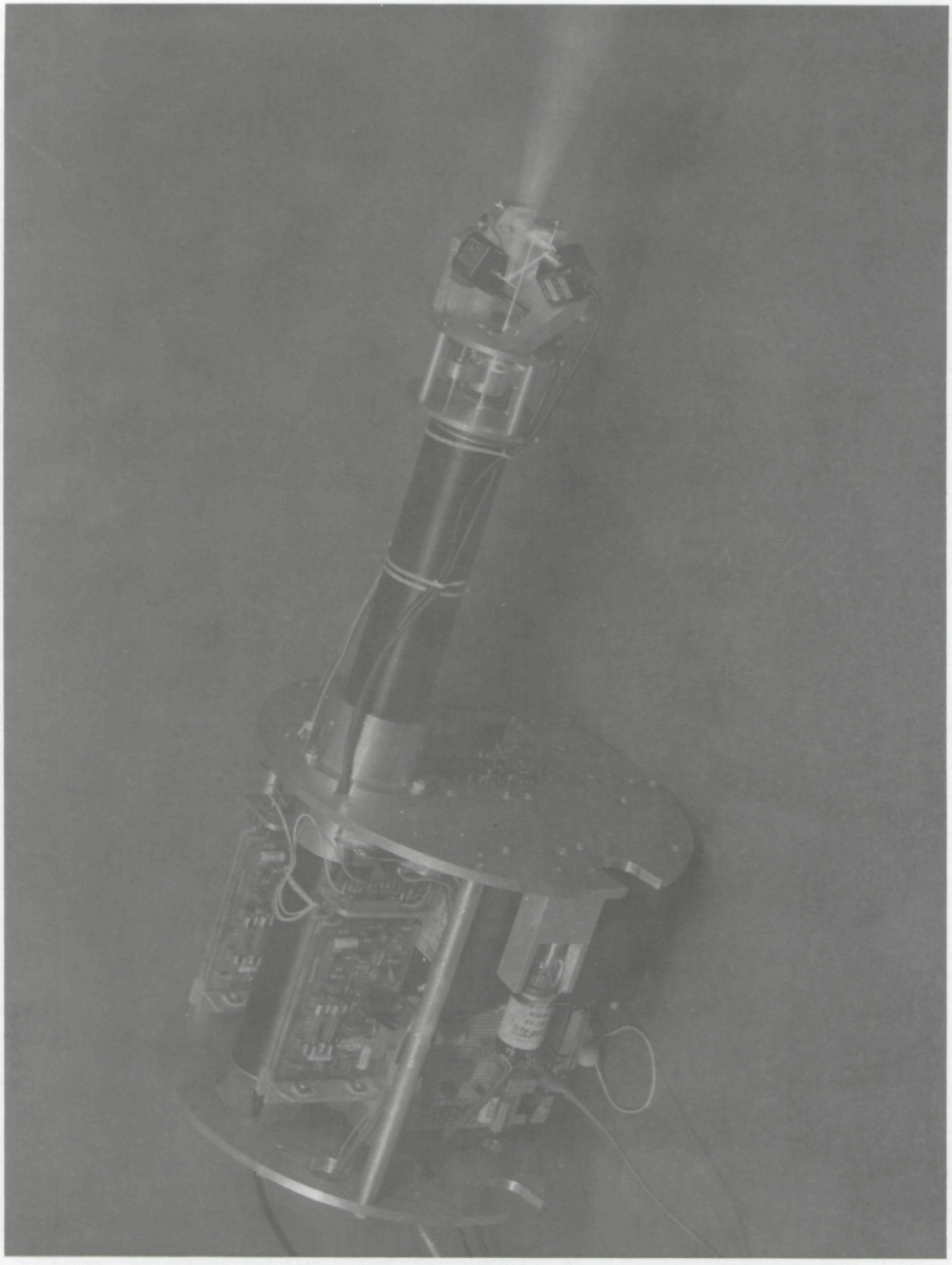

FIGURE 3. Photograph of underwater laser scanner unit (without underwater housing). The HeNe laser is seen mounted atop the electronics package, the sync pulse flash lamp (one of two) can be seen to the side of the electronics package and the scanning unit is attached to the output end of the laser. The laser beam can be seen traversing the scanning unit. The beam is first spread into a line by the horizontal (x-axis) scanning mirror and then spread into a square (raster) by the vertical (y-axis) scanning mirror.

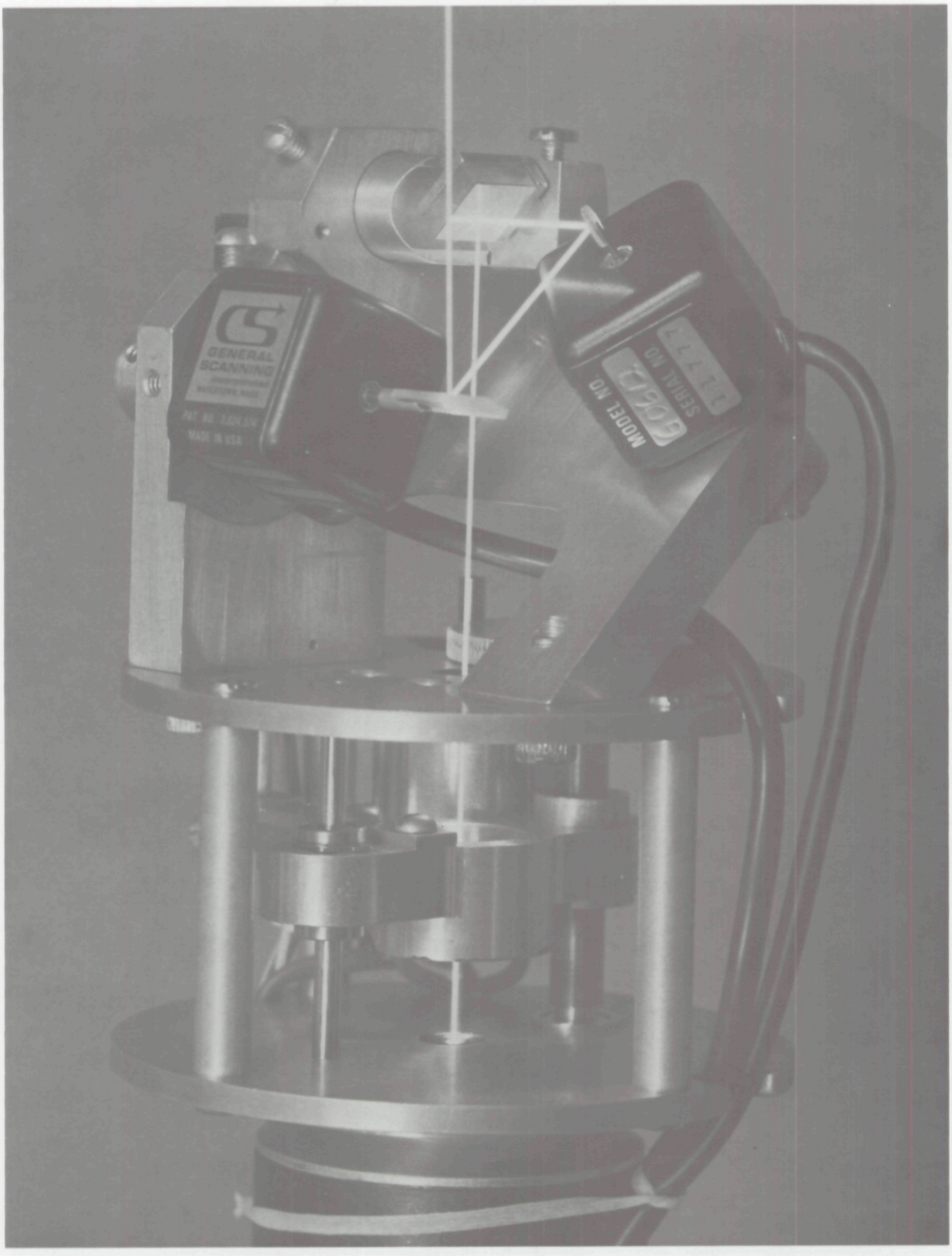

FIGURE 4. Photograph of the scanning unit. The laser beam can be seen emerging from the laser and passing through an adjustable lens. The beam is then reflected from a fixed front surface mirror to the horizontal (x-axis) and vertical (y-axis) scanning mirrors. The scanning mirrors are driven by low inertia high speed galvanometer drivers (black cubes).

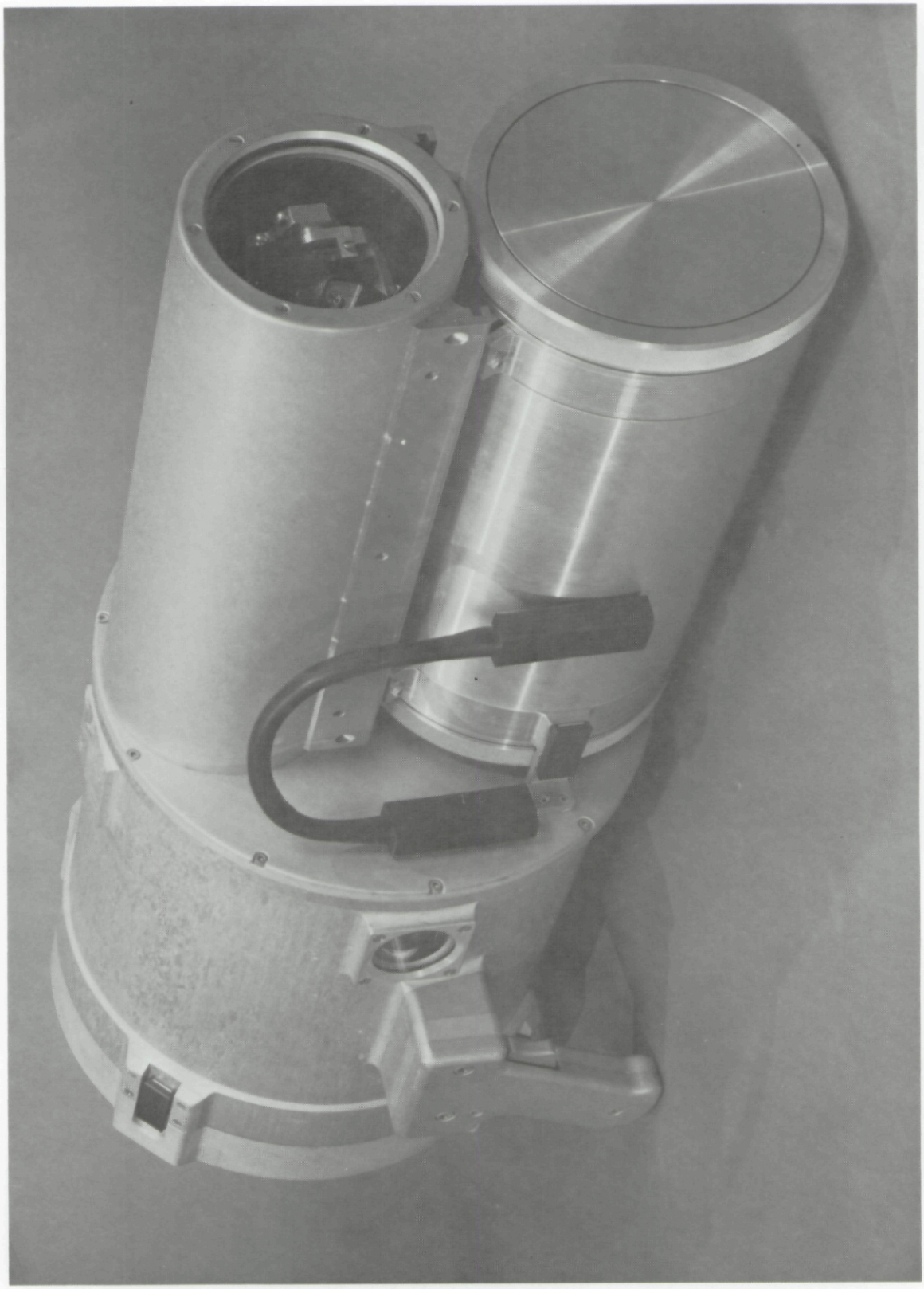

FIGURE 5. Photograph of underwater laser scanner unit in underwater housing.
(FIGURE 5 is a copy of FIGURE 14 in PART II)

element in a 256 x 256 array for 8 microseconds, then a line scan takes 2.048 milliseconds which is slower, as it must be, than the 1.85 millisecond ($=\frac{1}{540\ Hz}$) maximum frequency of the optical scanners. The full array would then take 0.524 seconds ($= 256 \times 2.048 \times 10^{-3}$). The scanning rate, which determines both the speed of a raster scan and the time spent illuminating each resolution element, is one of the limiting parameters of the present experimental TVI system.

Synchronizing Flashtubes

The synchronizing pulse, which initiates the time-encoded sequence of the laser scanner and receiver/display units, is provided by two spectrally filtered EG and G (Model No. FX-101) Xenon flashtubes. These small flashtubes have a long life (up to 10^9 flashes) and are capable of producing short duration, high radiance pulses. For the TVI system they have been filtered (Kodak Wratten filter No. 44, having a broad band centered about 490 nm) to place their output in a spectral region separate from that of the laser output and to maximize transmittance through sea water. Tests, described in Appendix B, show that these lamps are capable of providing a suitable sync pulse through nearly forty attenuation lengths of water. Thus, the sync pulse should never limit our TVI performance and evaluation tests.

Battery Pack

Silver-Cadmium batteries (Yardney Model BD 3/10) were chosen to power the underwater laser scanner unit. These batteries have a high energy density (nominal 30 watt-hour per pound), are rechargeable for several hundred cycles under normal use and have a relatively constant voltage output (compared to other types of batteries) over the discharge time of the battery (see Fig. B1 in Appendix B). The experimental TVI system uses 8 of the BD 3/10 SilCad batteries with a nominal rating of 10 ampere hours at 24.8 volts. This battery pack weighs 9.6 pounds and occupies 147 cubic inches (11-1/4" x 3-7/8" x 3-3/8"). Tests (see Appendix B) indicate that this battery pack will be capable of powering the underwater laser scanner unit for one to two hours on a single battery discharge cycle. Approximately 16 hours are required to recharge the battery pack. Two interchangeable battery packs have been acquired.

It should be noted that ultimately the output power and size of the underwater laser scanner unit are primarily dependent upon the efficiency of the laser used and the number and energy density of the batteries used. Thus, the choice of a maximum size for the underwater unit practically dictated the maximum output power, and hence operational range, of the system.

Electronics

The electronics in the underwater laser scanner unit were designed to be reliable, to be compact, and to have a low power consumption. In addition the circuitry for this experimental model was designed for ease of service, modification and evaluation. Principal electronic components in the underwater unit include: laser DC power supply; Xenon flash tube trigger transformers, flash control and high voltage supply; three basic logic boards which include the crystal oscillator, the X raster generator, and the Y raster generator; X and Y scanning amplifiers, galvanometer drivers and

galvanometers; a low voltage cutoff circuit; and a control panel. The control panel includes: a power on-off switch; a battery voltage indicator; a mode selection switch for continuous or single shot scanning; an adjustment for optimizing laser beam spot size; and a switch to select a wide or narrow angular field of view for the scan (the maximum angular field of view is 18° in water). These controls have been designed for ease of operation by a diver underwater, but they are primarily for test and evaluation purposes. Routinely a diver needs only to turn the power on, aim the laser scanner and pull a pistol grip trigger to initiate an imaging sequence.

Underwater Housing

The underwater housing for the laser scanner was designed to be contained (exclusive of handles) within a 24 inch long by 12 inch diameter volume. The design depth for this experimental unit is 100 feet.

As previously mentioned, a prime consideration in the configuration and design of the underwater unit was the ease of operation underwater by a diver. The underwater unit has a slight negative buoyancy, is balanced for ease of handling underwater, has no sharp or fragile protuberances, has controls which may be operated while wearing gloves, and has a single hand trigger for initiating a scan sequence. The battery pack, enclosed in its own underwater housing, may be easily removed from the remainder of the underwater laser scanner unit. In addition, the underwater battery housings may be exchanged while the unit is submerged. The battery pack has also been insulated (to contain its own dissipated heat) in order to maintain the batteries at a more efficient operating temperature.

The underwater housing is also designed for ease of testing and servicing the internal components. It has a quick release cover which allows the entire internal unit to be easily removed without breaking electrical connections. This feature allows the laser scanner unit to be tested and adjusted in the laboratory or on deck and then quickly, without any electrical changes, to be placed within the underwater housing. In addition, the underwater housing has been constructed of non-corrosive material and, for initial tests, has been provided with a tripod mount.

2) Receiver/Display Units

The receiver/display units of the TVI system are shown schematically in Fig. 1. These units, which remain with the operator monitoring the image display, are composed of an underwater receiver unit and a control/image storage/display unit. Two separate photomultipliers in the underwater receiver unit detect, respectively, the sync pulse and the time-encoded laser light reflected from the target. The control/image storage/display unit processes these received signals and provides storage and/or display of the received image.

Underwater Receiver Unit

The underwater receiver unit contains two appropriately filtered photomultiplier tubes (PMT) and associated electronics (Fig. 6). An important feature of the electronics is a DC to DC converter to provide high voltage to the photomultipliers from a low voltage input via an underwater cable. By limiting the underwater cable to low voltages the problems associated with high voltage underwater connectors are avoided. Both photomultiplier tubes are 2 inch diameter, 12 stage, head-on type PMT's with low dark currents and high quantum efficiencies. An RCA 4507 PMT is

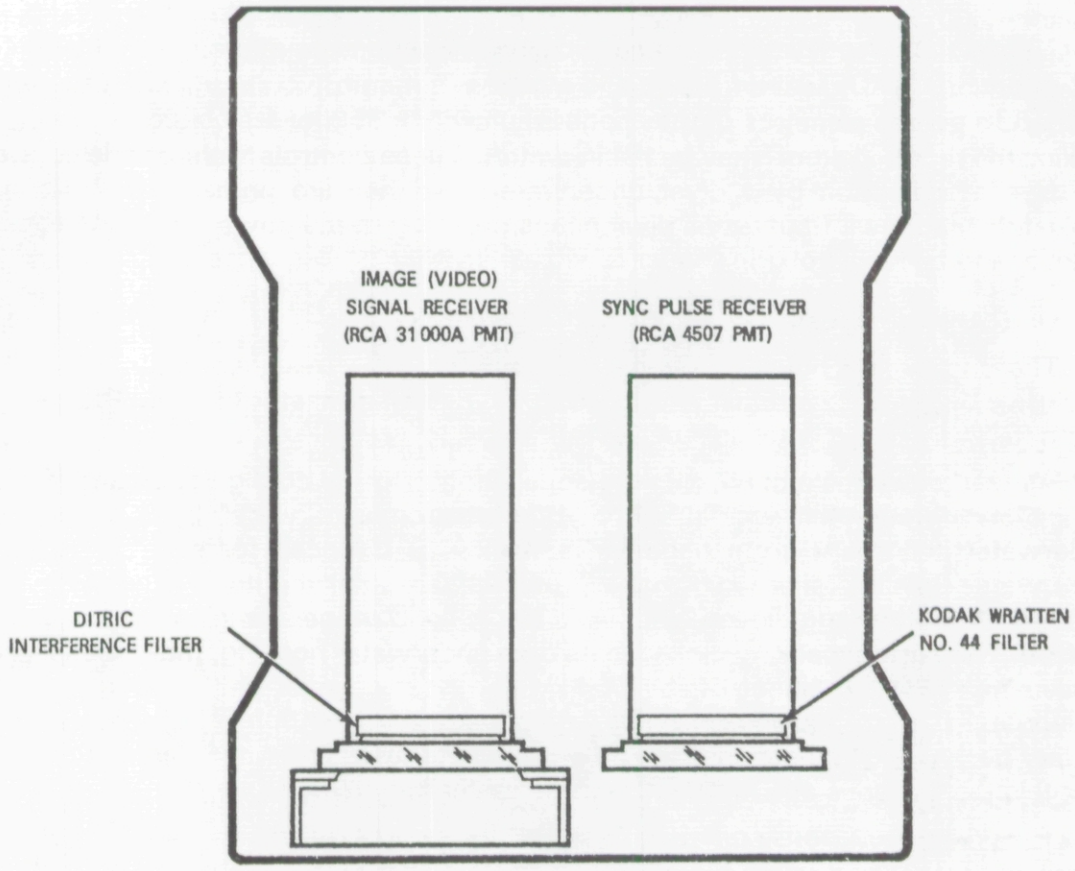

FIGURE 6. Schematic diagram of underwater receiver unit. The synchronization pulse is detected by an RCA 4507 photomultiplier covered with a Kodak Wratten No. 44 filter. The time encoded laser signal reflected from the target is detected by an RCA 31000A photomultiplier covered with a three cavity interference filter chosen to optimally pass the laser light at 632.8 nm.

used to detect the sync pulse. This tube, with a bialkali photocathode, has an extremely low dark current and high current amplification. The RCA 4507 is covered with a Kodak Wratten No. 44 filter so as to match the similarly filtered sync pulse of the Xenon flashtube. An RCA 31000A PMT, employing an extended red multi-alkali (ERMA) photocathode, is used to detect the time-encoded laser signal reflected from the target. This tube was selected to have greater than 7 percent quantum efficiency at 632.8 nm, the output wavelength of the HeNe laser. An interference filter, to block ambient light, covers this photomultiplier and effectively limits the received signal not only to a narrow spectral range (near 632.8 nm) but also limits the geometrical angle of acceptance to plus or minus 30° (see discussion and graph Appendix B).

Control/Image Storage/Display Unit

A photograph of the control/image storage/display unit is shown in Fig. 7. A signal flow diagram of the receiver/display system is shown in Fig. 8. In brief, the control/image storage/display unit, upon receipt of the sync signal, begins the

reception of the laser signal. This received signal, after passage through an analog to digital converter (ADC) is addressed and stored in a memory core organized to store the 65,536 picture elements of the image, each with a 256 level (8 bit) grey scale. In parallel, the received signal may be passed through a multiplexer to the scope control

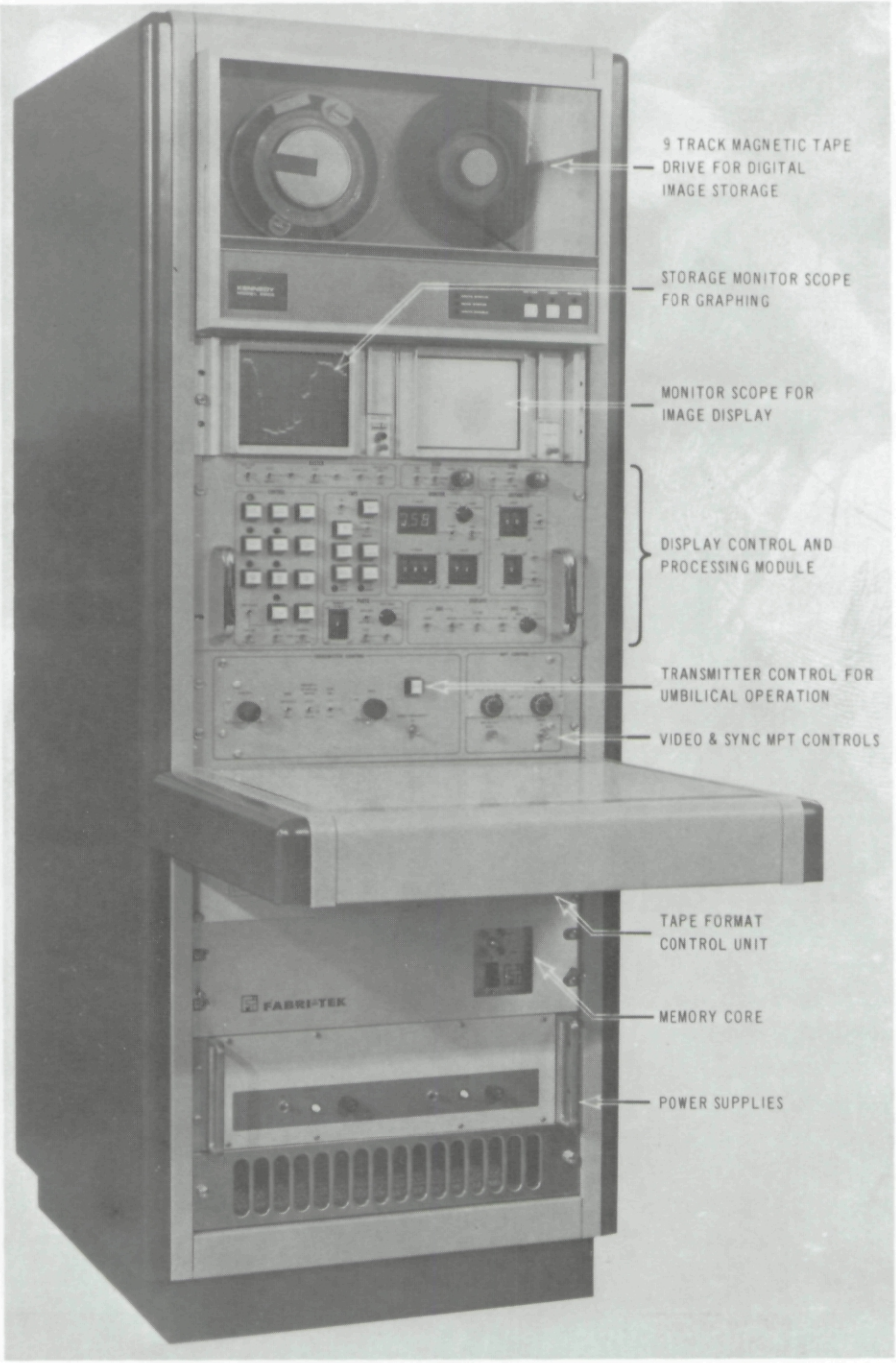

FIGURE 7. Photograph of control/image storage/display unit. Principal components are labeled on the figure.

for direct display on the oscilloscopes and possible photographing by polaroid camera. The signal image array may also be processed by the arithmetic unit, either directly or upon recall from storage. The arithmetic unit can be used to add or subtract or multiply the image array by constant factors. This allows the control

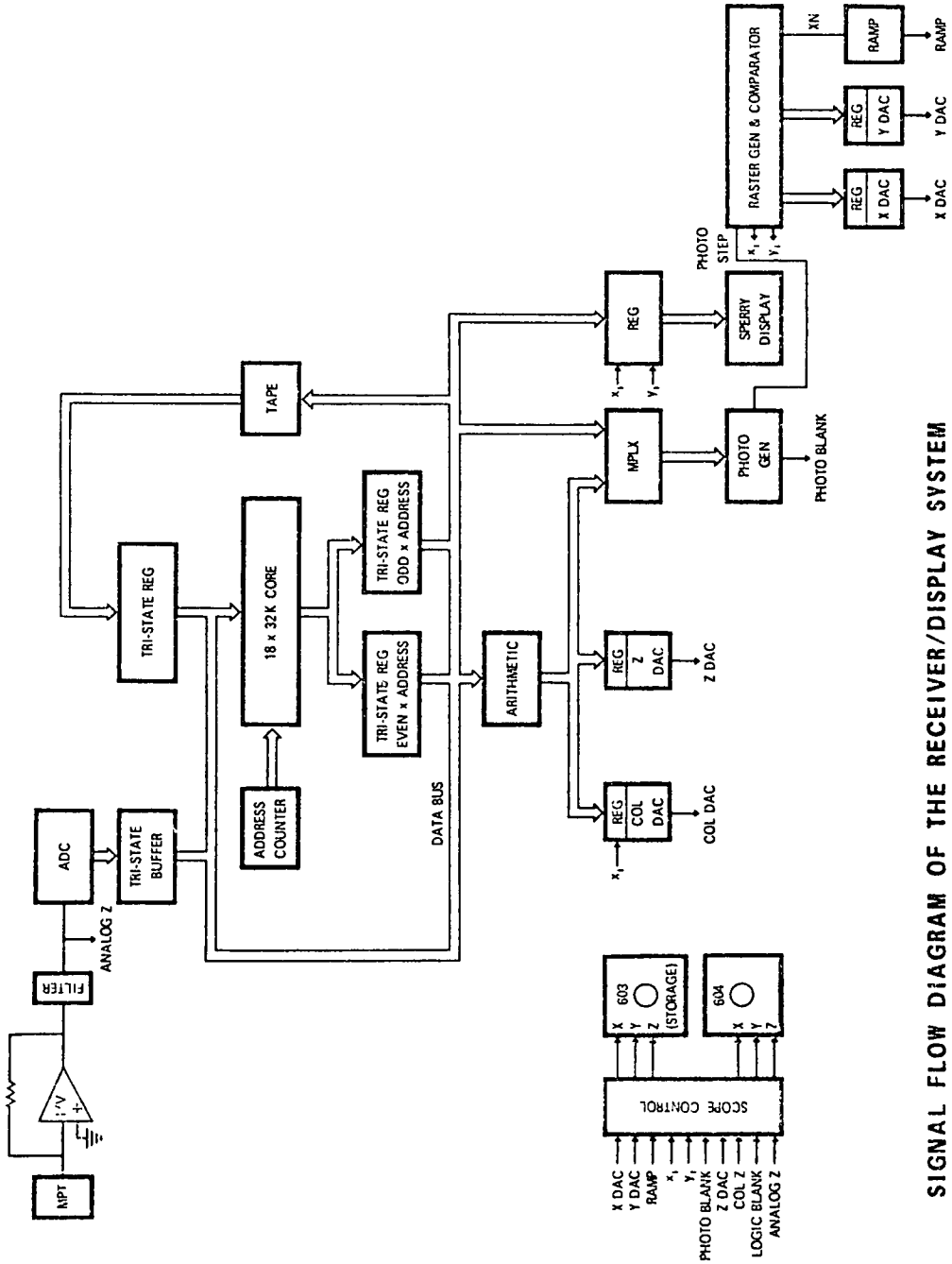

FIGURE 8. Signal flow diagram of the receiver/display system.

operator to adjust the image display for optimum contrast or to highlight a particular portion of the image for special observation. The image array may also be stored on, or recalled from, magnetic tape. This allows the control operator to rapidly store a series of images on magnetic tape and later to recall any of these images for detailed inspection and analysis. The image array may also be automatically recalled from core for continuous (refresh) display on the monitoring scopes. This allows the control operator to continuously view, or examine in detail, the desired image.

A primary consideration in the design of the control/image storage/display unit, beyond providing the basic components and controls necessary for underwater operating by a diver, was the provision of sufficient flexibility to allow engineers to make a full analysis of the TVI concept. Thus there are several functions which the unit can perform solely for the purpose of such analyses and a number of operational modes which provide this flexibility. The next section discusses the most important components of the control/image storage/display unit by tracing the various alternative pathways of an image array signal. A summary of parameters and modes of operation of the TVI system are given in a following section.

Alternative Pathways of Image Array Signal

As described above, a sync pulse from the Xenon flashtubes signals the initiation of a scanning sequence, the underwater laser unit scans the target and the image (video) photomultiplier tube (PMT) begins reception of the signal reflected from the sequentially illuminated resolution elements on the target. The video PMT anode current signal (see Fig. 8) passes through a current to voltage converter and a low pass filter which limits the signal bandwidth to one half the sampling rate. The signal at this point (called "analog Z") is an analog voltage proportional to the reflectance of a resolution element on the target. The time in the signal sequence with respect to the sync pulse determines the particular (x,y) coordinate of the resolution element.

Each sequential element of the received signal then passes through an analog to digital converter (ADC) and into a tri-state buffer. The latter acts essentially as a data switch, sending the incoming video signal directly to the memory core or to the data bus for subsequent distribution to either the arithmetic unit or the multiplexer (MPLX).

The memory core is provided by a Fabri-tek Model 684 high speed random access core memory system. Its full cycle speed is 650 nanoseconds with a 300 nanosecond access time which is adequate to handle the data rates of the experimental TVI system. A byte control feature allows the 18 x 32K core to be used as a 9 x 64K core, adequate to store a 256 x 256 array. That is, two data bytes are packed into one 18 bit core address and later unpacked, via the tri-state registers, to the original two data bytes. Thus the core capacity, as used, is 65,536 (256 x 256) 8 bit words. The core memory has a wide operating margin, provided by temperature compensation circuits, and a feature which saves the data in case of power failure. The memory core may be loaded directly, as the sequential data arrives, or from data previously stored on magnetic tape.

The control/image storage/display system utilizes a Kennedy Model 9800 synchronous digital magnetic tape unit. This tape unit, along with the Kennedy Model 8212 formatting control, is capable of reading and writing tapes that are compatible with the Visibility Laboratory's IBM 360 computer 9 track tape units. Tape speed is

25 inches per second. The data rate is 20 k Hz at 800 characters per inch. This allows a 256 x 256 image array to be stored on tape in less than 4 seconds. With these units a 1200 foot magnetic tape has the capacity to store nearly 150 256 x 256 image arrays and attendant record gaps and file marks. Figure 7 is a photograph which shows the logic control panel, including magnetic tape controls.

From the data bus, which carries data directly via the tri-state buffer or from the memory core, the image array may be fed to the arithmetic unit, the multiplexer or the register which allows an individual resolution element to be read on a numerical (Sperry) display. The arithmetic unit allows any number to be added or subtracted from the array or the multiplication of the array by factors of two. This feature, for example, allows a DC level to be subtracted from the image array for possible enhancement of signal contrast and recognition. The register to the Sperry display allows a digital readout, by means of thumbwheel selection of X-Y coordinates, of the intensity (the Z value) of any individual resolution element within the array. Both of the above features provide operating flexibility for the engineering analysis of the TVI system. The multiplexer (MPLX in Fig. 8) provides the switching logic necessary to obtain the various input signals for the two monitor oscilloscopes.

Two display oscilloscopes are employed in the control/image storage/display unit, a Tektronix 603 Storage Monitor and a 604 Monitor (non-storage). Both are general purpose X-Y monitors which provide display (and storage with Model 603) of analog data. Analog inputs to the scope control for all display axes (vertical, horizontal and intensity) are obtained from the logic circuitry as shown on the signal flow diagram in Fig. 8. The analog Z (intensity) signal may be obtained directly (i.e., prior to entering the logic circuitry) or via, the memory core and the arithmetic unit. Analog X and Y signals are obtained from the logic system which decodes the time sequence of the image signal. In addition, for enhanced picture quality at high scanning rates, the analog X signal (comprising a series of discrete voltage steps) is replaced by a continuous ramp function. Also, by means of thumbwheels on the logic control panel, a single row or column of the image array may be selected from the 604 display monitor for a graphical display of signal amplitude versus row or column position on the 603 storage monitor.

A Tektronix C-5 camera, utilizing a Polaroid Land film pack, may be used with either scope to photograph a display. For this purpose it is desirable to produce a display whose brightness is linearly proportional to the input intensity. The Photo-Generator, of the logic circuit, creates a pulse whose width is proportional to the intensity of each resolution element. Using this pulse the voltage to the cathode ray tube (CRT) grid is held constant while the dwell time is proportional to intensity (analog Z). In this way the nonlinearity associated with variable CRT voltages is avoided.

While the underwater laser scanner unit is battery powered and self-contained it is also possible to operate this underwater transmitting unit by means of an umbilical cable. This additional flexibility will be useful for initial testing and evaluation, where the use of batteries is unnecessarily restrictive. The transmitter control panel, in the control/image storage/display unit, provides local control of the laser scanner unit when it is attached by the umbilical cable. In addition to the diver controls, discussed

above, three raster sizes (256 x 256, 512 x 128, or 1024 x 64 horizontal x vertical picture elements), scan times of 0.5, 1 and 2 seconds and a continuous focus of the laser beam are provided by the transmitter control.

The control/image storage/display unit also contains the controls for adjusting the high voltages to the two photomultiplier tubes (labeled MPT control) in the underwater receiver unit. These controls allow an operator to optimize both the size of the sync pulse and the video signal received from the laser scanner.

Because of the wide flexibility of the control/image storage/display unit it is impractical, in this report, to attempt a description of all possible operational and test procedures. In the following section a summary of important parameters and an outline of the various operating modes of the TVI system are given.

C. TVI System, Summary

1) Component Parameters

a) Laser (Coherent Radiation Model 80-6 HeNe),

output power	- 6 milliwatt (CW, TEM_{oo}, unpolarized)
wavelength	- 632.8 nm
beam diameter	- 0.7 mm @ $1/e^2$ points
beam divergence	- 1.15 milliradians
rms noise	- less than 0.2% (1 Hz - 2 M Hz)

b) Optical Scanners (General Scanning Inc. Model G-0612)

X axis mirror	- 5.0 mm diameter x 0.5 mm
	- 669 Hz (70% duty cycle)
Y axis mirror	- 4.0 mm x 15 mm x 1 mm
	- 514 Hz (70% duty cycle)
maximum scan rate	- 0.5 seconds for 256 x 256 array (pixel rate 8μ sec)
angular field of view	- adjustable, ± 12° maximum in air (±9° in water)

c) Battery Pack (Yardney Model BD 3/10)

nominal rating	- 10 amp hours @ 24.8 volts
testing rating	- 7.65 amp hours @ 24.9 volts (5 amp discharge rate @ 20°C)
weight	- 9.6 pounds
volume	- 147 cubic inches (11-1/4" x 3-7/8" x 3-3/8")

d) Underwater Receiver

sync pulse receiver	- RCA 4507 photomultiplier plus Kodak Wratten No. 44 filter
image signal receiver	- RCA 31000A photomultiplier plus Ditric bandpass interference filter
	- quantum efficiency greater than 7% @ 632.8 nm
	- geometrical angle of acceptance ±30°

e) Memory Core (Fabri-tek Model 684)

storage capacity	- 65,536 x 8 bit
full cycle time	- 650 nanoseconds
access time	- 300 nanoseconds

f) Magnetic Tape (Kennedy Model 9800 tape & Model 8212 formatter)

formatting	- IBM compatible
tracks	- 9
speed	- 25 inches per second
density	- 800 bits per inch
data rate	- 20 K Hz at 800 bits per inch
tape capacity	- 149 arrays (256 x 256 + record gaps and file marks) on 1200 foot reel

2) Control/Image Storage/Display Unit Parameters

a) Memory storage capacity - 65,536 x 8 bit

b) Raster Size
i) 256 x 256
ii) Arrays of 1024 x 64, 512 x 128, or 256 x 256 may be stored.
iii) Automatic gain adjustment with manual override.

c) Z Axis (intensity)
i) 8 bits (1 part is 256) resolution
ii) In refresh mode the refresh display is amplitude modulated. For photo taking time gate modulation is used for linearity.
iii) Video processing during refresh. A constant value may be added to or subtracted from the digital video signal. The signal values may also be multiplied by factors of 2^N (N= 1,2,...) with or without displaying values in excess of 256. The values in excess of 256 may be displayed by intensity folding which provides a presentation similar to density contouring. In addition, the video signal may be inverted to provide a negative image of the scene.

d) Scan Rate - a 256 x 256 element array can be scanned in 0.5, 1.0 or 2.0 seconds (Pixel durations of 8, 16, or 32μ seconds).

e) Refresh Rate - 30 frames/second, interlaced or non-interlaced or 45 frames/second non-interlaced.

f) Photographs
i) Scan mode; amplitude modulated directly from incoming signal or time gated with 1 part in 128 resolution.
ii) Slow core cycle mode: resolution can be varied from 256 to 64 in factors of 2. Conversion clock can be varied from 8 M Hz to 1 M Hz in factors of 2.

g) Tape Reading or Writing - less than 4 seconds per 256 x 256 array.

3) Control/Image Storage/Display Unit Modes

a) Scan
i) An amplitude modulated or time gated picture is always produced on the refresh monitor for visual monitoring or photographing.

ii) The "graphing scope" (#603 Storage Monitor) can present the following:

- any row as a graph of pixel intensities versus position in the row, row selectable by thumbwheel switches.
- any column as a graph of pixel intensities versus position in the column, column selected by thumbwheel switches.
- the entire scan (in this mode each row is reduced to a point).
- an isometric display presenting the X, Y, Z information for the entire image as a surface.

iii) The intensity value at any point can be read out on the Z axis monitor (Sperry display). A reading may also be made on all incoming points to facilitate the signal PMT high voltage setting.

iv) The memory core may or may not be loaded during the scan, at the discretion of the operator.

b) Refresh

i) The memory core is cycled at a 30 Hz rate to provide either an intensity modulated or an isometric picture on the display scope (#604 non-storage monitor).

ii) The graphing scope (#603) can show a graph of any row or column as in (3a, ii) above.

iii) The Z axis monitor can display any single intensity value.

iv) The display scope has the following marker selection:

- a vertical or horizontal line of either a row or a column is selected for the graphing scope.
- both the above (i.e., row and column) with their intersection being the Z axis display point selected by the thumbwheel switches.
- no marker
- the marker can be selected to be bright or dark or to alternately bright and dark.

c) Photo

The memory core is cycled at a selectable rate and time gated modulation appears on both scopes.

d) Graph

The memory core is cycled at a slow rate and the graphing scope can display a graph of any row or column or an isometric picture.

e) Write Tape

The memory core is cycled at the tape read/write clock rate and the data array in memory core is written on tape. Both displays are time gate modulated and a raster is scanned in synchronism with the tape.

f) Read Tape

A file is read from tape and loaded into core. Display presentations are the same as in the write tape mode.

D. Design Considerations

1) Theoretical

In Appendix A a calculation of the received video signal strength of a TVI system is given. The principal result is given by Eq. (A-11).

$$N = P_1 \bullet \rho \bullet \frac{D_R^2}{4} \bullet \frac{\Delta t}{q} \left\{ \eta_R(\lambda) \bullet \frac{e^{-\alpha(\lambda)(r_1 + r_2)}}{r_2^2} \left[1 + \frac{K(\lambda) r_2}{2\pi} e^{(\alpha(\lambda) - K(\lambda)) r_2} \right] \right\}$$

where

N	=	the number of electrons per resolution element comprising the receiver photomultiplier current (i.e., a measure of the received signal).
P_1	=	laser output power (CW) (i.e., the input signal).
ρ	=	target reflectance.
D_R	=	effective diameter of receiver.
$\eta_R(\lambda)$	=	photocathode efficiency of the detector.
Δt	=	interval of time the laser scanner irradiates each resolution element.
q	=	charge on an electron.
e	=	base of natural logarithms.
r_1	=	laser scanner-to-target distance.
r_2	=	target-to-receiver distance.
$\alpha(\lambda)$	=	volume attenuation coefficient.
$K(\lambda)$	=	diffuse attenuation coefficient for irradiance.

Several design considerations are evident from the above equation. (1) The received signal is directly proportional to the signal input. The greater the laser power the greater the received signal. (2) The effectiveness of the receiver is increased as the square of the diameter of the detector and proportional to the photocathode efficiency. (3) The received signal is proportional to the time interval, Δ t, the laser scanner irradiates each resolution element. This time interval is proportional to the scan rate and inversely proportional to the raster array size. Thus faster scanning rates and larger raster arrays both reduce the received signal.

The key to the TVI system operation is also contained in the above equation. The first term in the square brackets [ ] represents the monopath component which is the only light flux useful in conventional imaging systems. The second term yields the magnitude of the multipath or scattered light component which in the TVI system also contributes useful signal flux. In conventional systems this second component is a masking flux and contributes only to the system noise. The relative magnitudes of these two terms depends upon the relative values of α and K. In turbid waters, where the attenuation is dominated by a large scattering coefficient, the second term can

become orders of magnitude larger than the first. This is precisely the situation in which conventional imaging systems are most limited and, thus, the TVI system has its greatest advantage.

The curly brackets { } contain the terms which are dependent upon wavelength. We assume that the receiver photocathode efficiency will be chosen to optimally match the wavelength output of the laser. The remaining wavelength dependencies are a function of the optical properties of the water surrounding the TVI system.

Numerical calculations, and the graph (Fig. A2), given in Appendix A confirm the intuitive notion that the optimum wavelength for a TVI system (as for any imaging system) is the wavelength of maximum transmittance for the water in question. Since turbid waters present the most severe restrictions upon imaging systems and since these waters have their maximum transmittance in the green portion of the spectrum we can conclude that an optimum choice of wavelength for a TVI system would be in the green spectral region. It should be noted however, from Fig. A2, that adequate signals may be received using red light ($\lambda = 630$ nm) out to 15 attenuation lengths (in this case the ratio of multipath to monopath light flux is several thousand to one).

2) Previous Experimental Trials

The theoretical design considerations discussed above have been experimentally tested using a breadboard TVI system in a 13-meter long tank at the Visibility Laboratory. A schematic diagram of the breadboard laser scanner is shown in Fig. 9. Both blue light from an argon-ion laser (488 nm) and red light from a helium-neon laser (632.8 nm) were employed at different times during these early trials. The raster scan was provided by a pair of orthogonally oriented mirrors mounted on high speed galvanometer armatures. The scanning beam passed through either a one-half, one or two meter path of water to various two and three dimensional submerged objects, e.g., resolution charts, grey scales, diver's wristwatch, a register counter, etc. The light reflected from these objects traversed the entire length of the tank (12.7 meters) to a photomultiplier tube mounted in an underwater housing. The absorption and scattering properties of the water in the tank were measured and varied over wide ranges through the use of additives and by filtering. Trials were also made using freshly collected coastal sea water with nearly identical results.

The output of the photomultiplier was used to intensity modulate a cathode ray tube display monitor which was deflected in synchronism with the scanner. Polaroid photographs of the display monitor were obtained to provide a record of the image quality.

These tests demonstrated the basic TVI concept under laboratory conditions. It was found, from depth of field tests, that the system suffered no loss of resolution due to laser beam spread over a range of scanner-to-target distances from 1/2 to 2 meters. In these tests resolution was found to be better than one line pair per millimeter *at the object*. Also, the theoretical design considerations (discussed in Section II D1 and in Appendix A) giving the relationships between image quality (i.e. image signal-to-noise ratio) and laser beam power and scanning ratio were found to be correct.

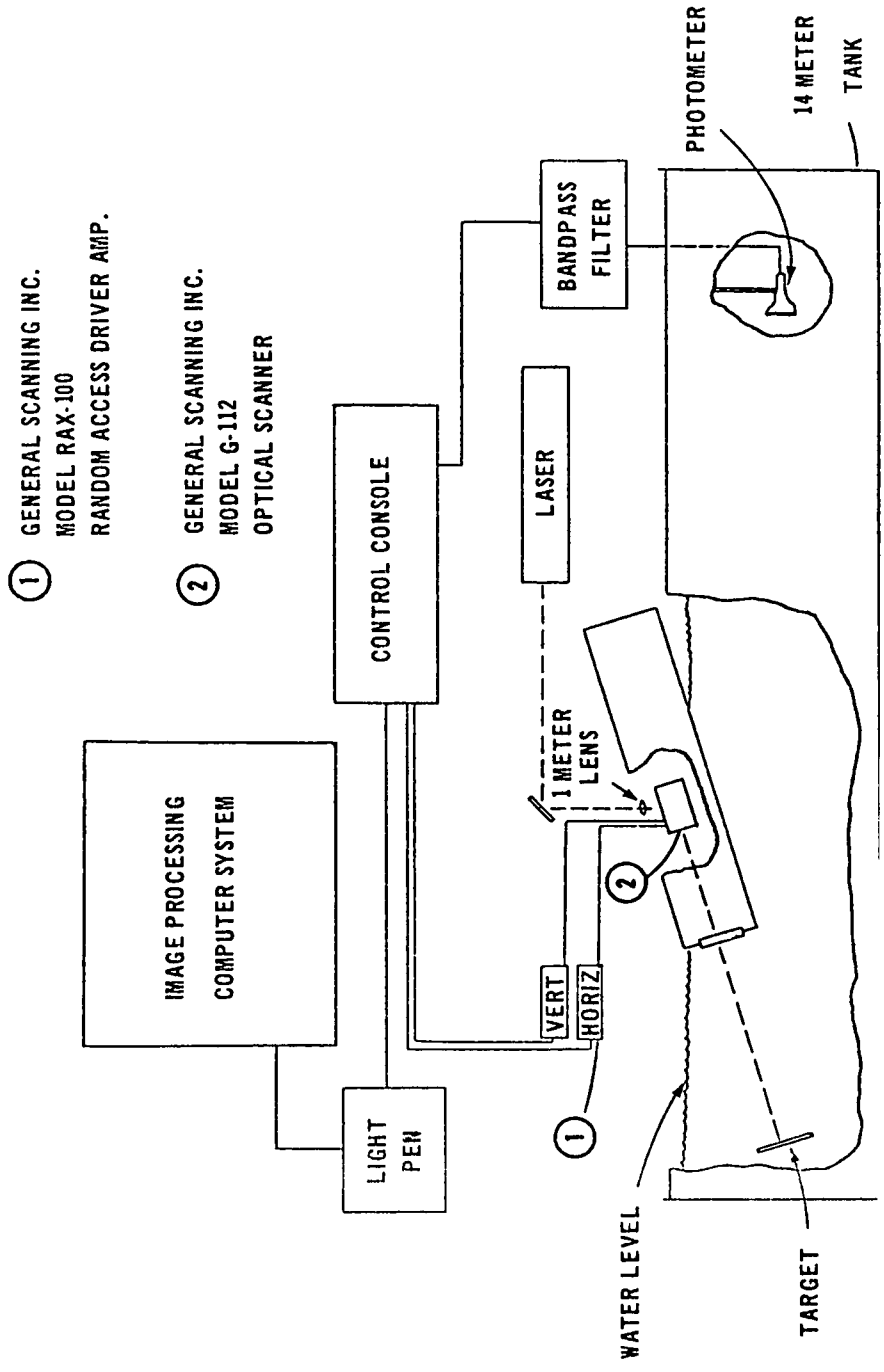

FIGURE 9. Schematic diagram of breadboard TVI system.

Most important, useful images were obtained of all target objects with various scanner and receiver distances using water with attenuation lengths ($1/\alpha$) as small as 0.25 meters. A selection of test results are shown in Figs. 10 through 13. It should be emphasized that Figs. 10 through 13 represent tests using a breadboard TVI system in the laboratory. These tests were used to obtain information necessary for the construction of the experimental TVI system. Tests of the experimental TVI system are discussed in a later section (III) of this report.

FIGURE 10. Images obtained using breadboard TVI system. In this, and the following three figures (which are photographs of photographs of oscilloscope displays), the captions below individual images give: the wavelength of laser emission, in nanometers; the laser scanner-to-target distance (r_1) and the target to receiver distance (r_2), in meters; the array size of the raster scan; the attenuation length (1/α) of the water, in meters. The laser power *(P_1) for the blue (488 nm) laser was 40 milliwatts and 0.5 milliwatts for the red (632.8 nm) laser. The scanning rate was 1 second for each 64 x 64 picture elements in an array.*

This figure shows a series of images of a small register counter. (The front dimension of this counter is 1.65 inches (4.2 cm), the side 1.50 inches (3.8 cm) and the height 2.32 inches (5.9 cm). The "zeros" in the counter have an outside diameter of 0.18 inches (0.42 cm)). The left-hand images were scanned with a wide laser scanning angle while those on the right with a narrow scanning angle and r_1 was varied while holding other parameters constant. See discussion in text for details.

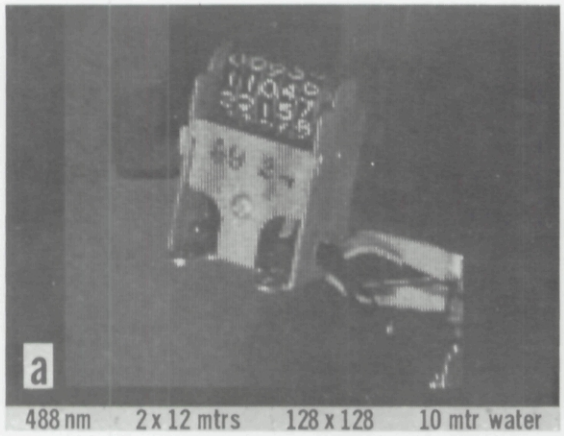

a

488 nm 2 x 12 mtrs 128 x 128 10 mtr water

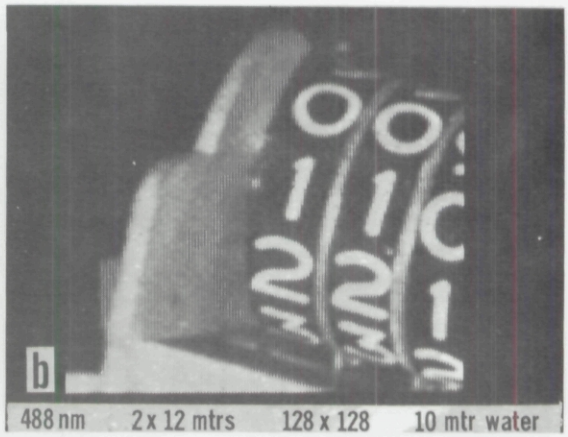

b

488 nm 2 x 12 mtrs 128 x 128 10 mtr water

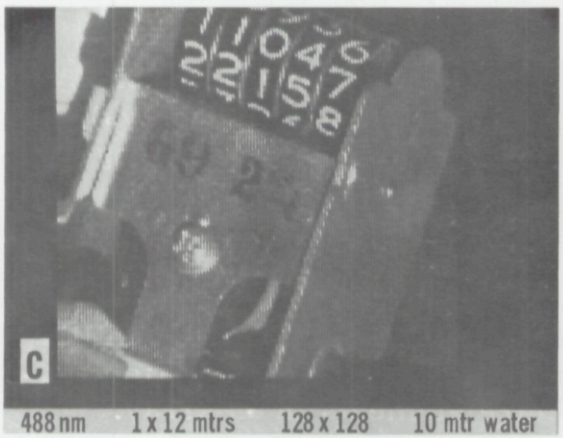

c

488 nm 1 x 12 mtrs 128 x 128 10 mtr water

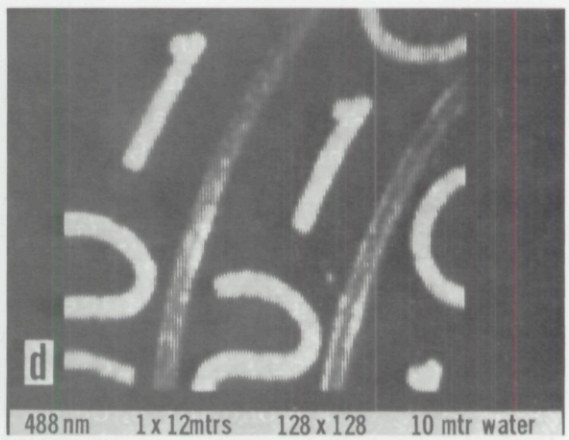

d

488 nm 1 x 12mtrs 128 x 128 10 mtr water

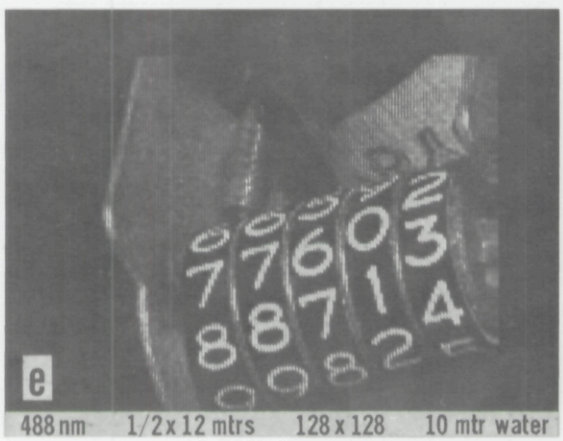

e

488 nm 1/2 x 12 mtrs 128 x 128 10 mtr water

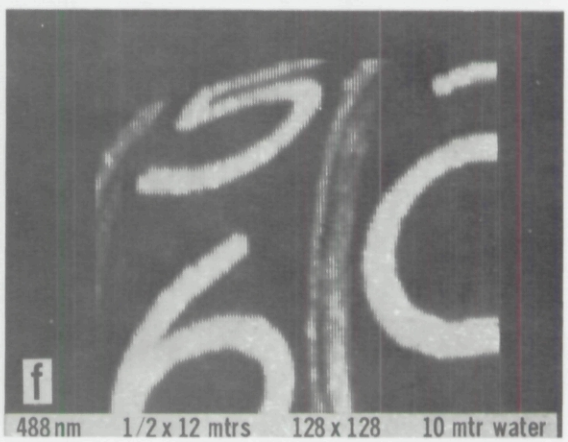

f

488 nm 1/2 x 12 mtrs 128 x 128 10 mtr water

Figure 10 shows a series of polaroid photographs of TVI images of a small register counter. In this figure the attenuation length of the water, the array size of the raster scan and the target-to-receiver distance are held constant for the six images shown. The laser scanner-to-target distance (r_1) was varied from 2 meters for the top images to 1/2 meter for the bottom images. Images on the left-hand side (a, c and e) were scanned with a wide laser scanning angle and those on the right-hand side (b, d and f) with a narrow laser scanning angle. In progressing from the top images to the bottom, i.e., as r_1 is decreased, a smaller area of the target object is scanned and hence a more detailed image of the object is obtained. Similarly, the images scanned with a smaller overall scanning angle (right-hand images b, d and f) but the same array size show a more detailed view of the object. Resolution of the wide scanning angle images (a, c and e) is limited by number of resolution elements in the array. This is because the angular distance between picture elements of the array is larger than the angular beam spot size of the laser, and thus the distance between picture elements determines the resolution. Conversely, resolution of the narrow scanning angle images (b, d and f) is limited by the laser beam spot size, since the angular spot size is larger than the angular distance between picture elements. In this case the size of the laser beam determines the resolution.

In Fig. 11 the attenuation length of the water has been varied, from 10 meter water to 0.67 meter water, while holding all other parameters constant. As in Fig. 10, the left-hand images were obtained with a wide laser scanning angle and the right-hand images were obtained with a narrow scan angle. Two processes are involved in the increasing degradation of these images as the attenuation length ($1/\alpha$) of the water is decreased. First, with reference to Eq. (A-11), as α is increased the signal-to-noise ratio of the received signal is decreased because fewer information carrying photons reach the receiver (thus reducing the number of photoelectrons per picture element, N). Second, as αr_1 increases there is an increase in the backscattered, non-information carrying light. This relatively constant (D.C.) background level (which also has a noise level associated with it) may be subtracted from the received signal, but this subtraction becomes increasingly less effective with increasing background inasmuch as the noise component remains after the D.C. signal has been removed. Note that images (e) and (f) were obtained with nearly 18 attenuation lengths of water between the target and receiver (αr_2).

Figure 12 shows four polaroid photographs of TVI images of a diver's watch. The laser scanning angle has been progressively narrowed to show increased detail of the watch while all other parameters were held constant. These photographs convincingly demonstrate that high quality images can be obtained through 24 attenuation lengths of water. Dimensions of this watch are: outside diameter of movable bezel, 1-1/2 inches; diameters of inner lapse time dials, 5/16 inch; height of numbers on bezel, 3/32 inch; height of numbers on watch face, 1/16 inch; height of numbers on lapse time dial, 1/32 inch; height of letters in word "ARDATH," 1/32.

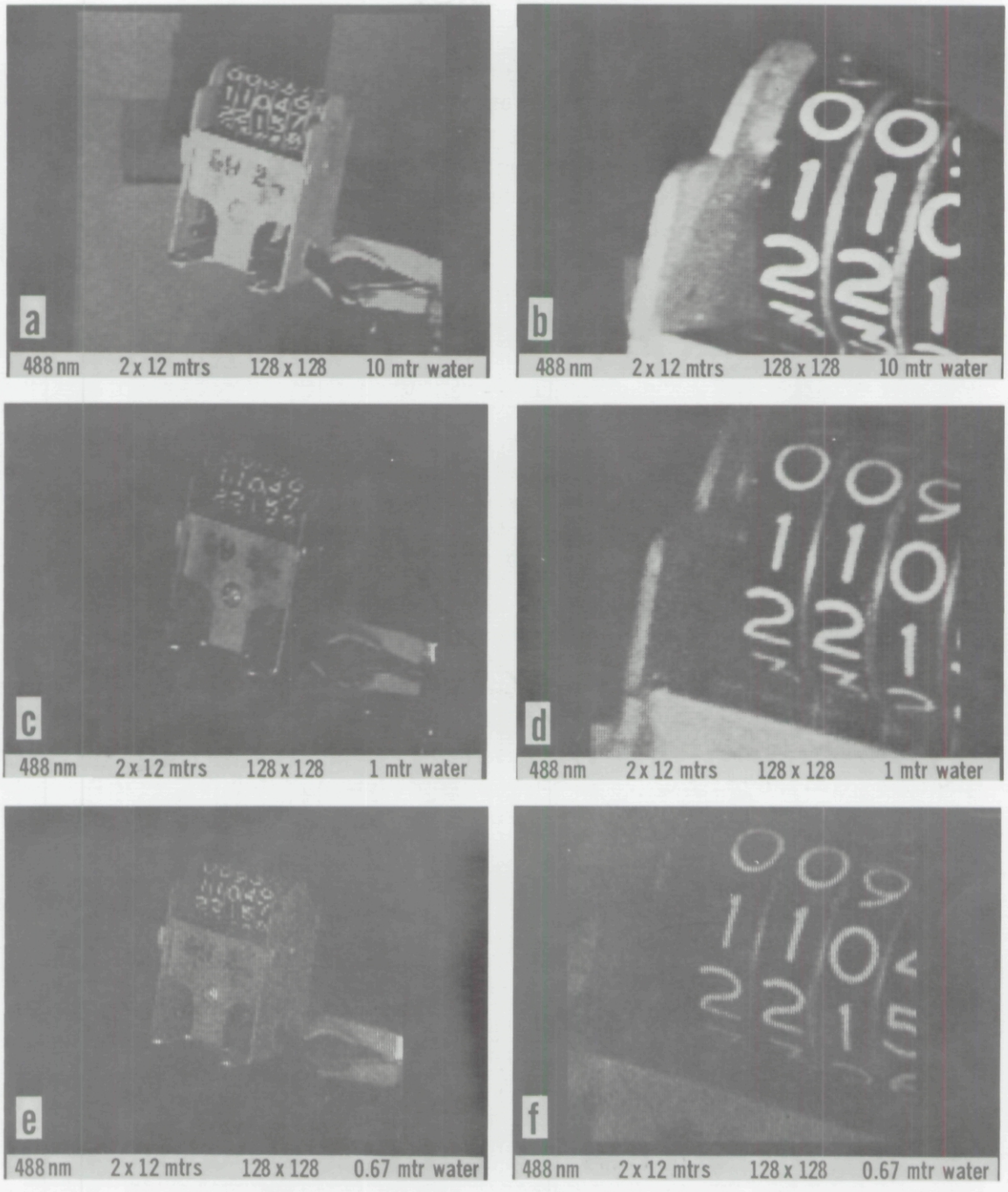

FIGURE 11. Images using breadboard TVI system. In this figure the left-hand images were scanned with a wide scan angle while those on the right were scanned with a narrow scan angle and α was varied while holding other parameters constant. See discussion in text for details.

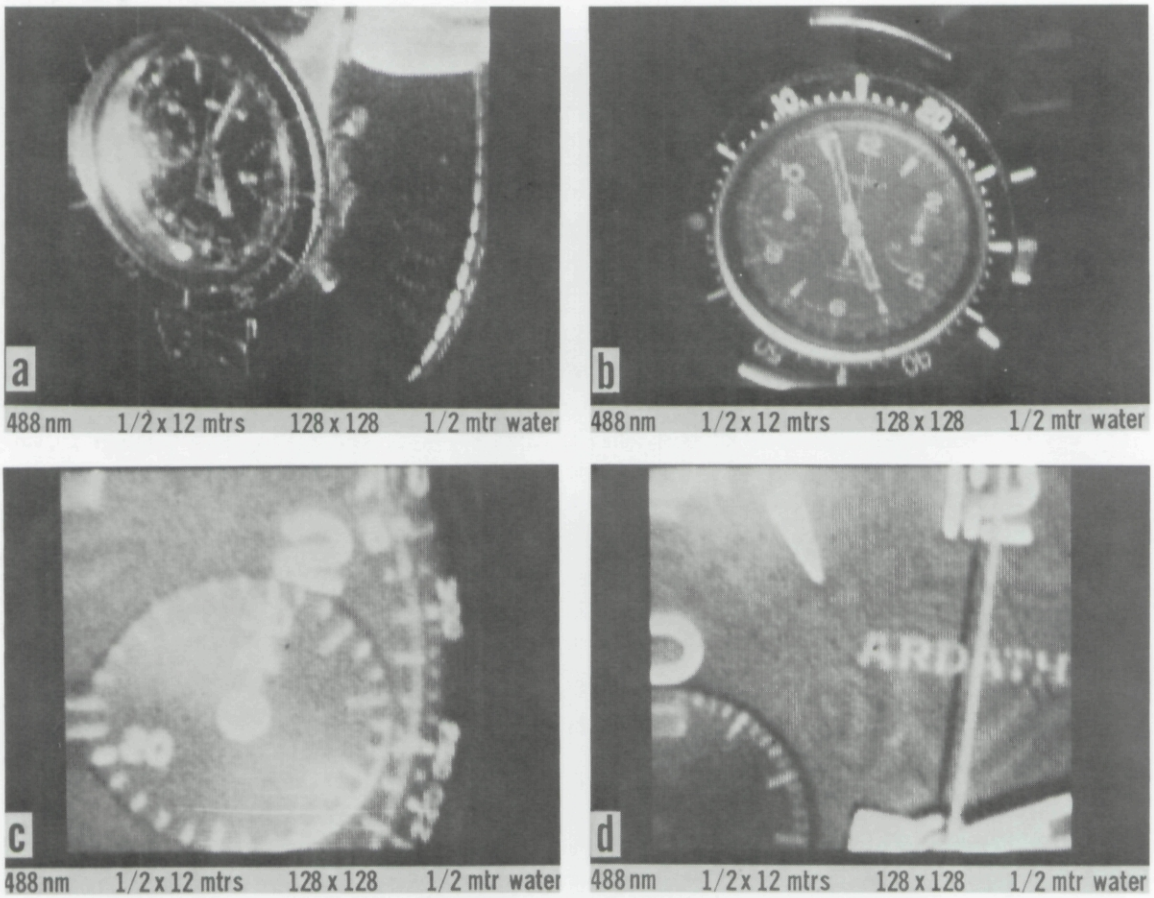

FIGURE 12. Images obtained using breadboard TVI system through 24 attenuation lengths (αr_2) of water. These photographs convincingly demonstrate that high quality images may be obtained through many attenuation lengths of water. Dimensions of this watch are: outside diameter of movable bezel, 1-1/2 inches; diameter of inner lapse time dials, 5/16 inch; height of numbers on bezel, 3/32 inch; height of numbers on watch face, 1/16 inch; height of numbers in lapse time dial, 1/32 inch; height of letters in word "ARDATH," 1/32. See discussion in text for details.

Figure 13 shows a series of polaroid photographs of TVI images obtained using a 0.5 milliwatt HeNe laser (632 nm) in the breadboard set up. Note that high quality images have been propagated through 12 attenuation lengths of water using this 0.5 milliwatt red laser. A comparison of photographs (a) and (b) with (c) and (d) shows the degradation in image quality due to decreased signal-to-noise ratio as the attenuation length ($1/\alpha$) of the water is decreased. Note that image resolution was not, per se, degraded as the number of attenuation lengths (αr_2) between the target and receiver was increased from 6 to 12. Images (c), (d), (e) and (f) were all obtained through 12 (αr_2) attenuation lengths of water, however for images (e) and (f) both $1/\alpha$ and r_2 are one-half the values for images (e) and (d). While the total number of attenuation lengths (αr_2) was held constant for these images, the relative values of scattering (s) and absorption (a) coefficients, and hence the scattering and absorption lengths (i.e., 1/s and 1/a), were not. Images (c) and (d) are degraded (lower signal to noise ratio at receiver) with respect to images (e) and (f) because they have a lower scattering-to-absorption (s/a) ratio.

This comparison demonstrates that image degradation, for the TVI system, is primarily due to absorption rather than scattering. System limitations due to absorption can be overcome by increasing power. This is not true for limitations due to scattering. Thus, in marked contrast to conventional systems limited by scattering, image degradation in a TVI system can be eliminated by increasing laser power and images can be improved by optimizing wavelength transmittance, slowing the scan rate, using multiple receivers, etc.

The TVI breadboard system was also used to obtain images through sea water with results which were nearly identical to those for fresh water.

The breadboard results outlined above demonstrated the basic TVI concept under laboratory conditions. In addition, they provided experience and design information for the development of the present experimental TVI system.

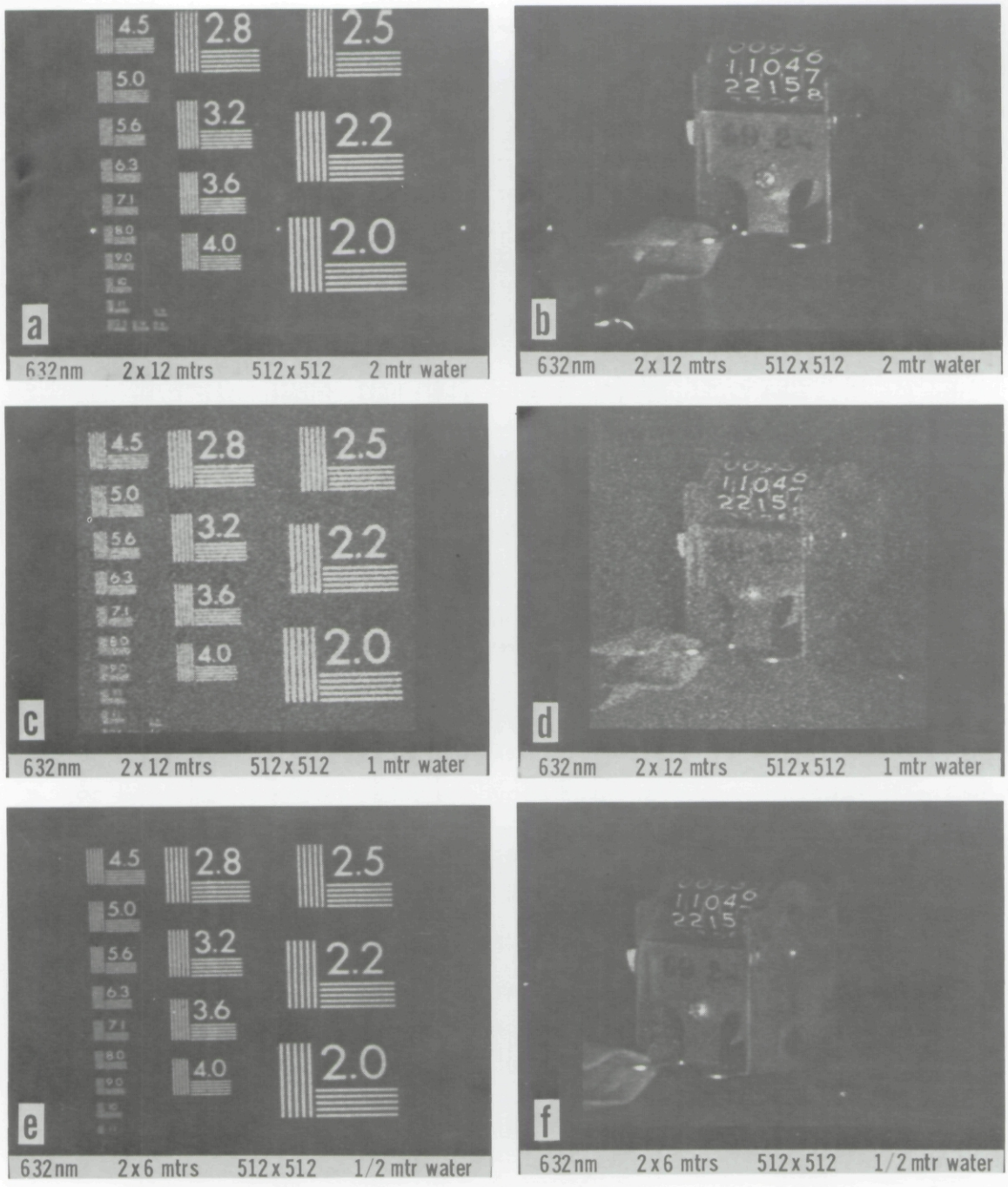

FIGURE 13. Images obtained using breadboard TVI system with an 0.5 milliwatt HeNe laser (632.8 nm). These photographs demonstrate that high quality images can be propagated through at least 12 attenuation lengths of water using a low power red laser. In this figure r_2 and α were varied while holding other parameters constant. See discussion in text for details.

TVI REPORT APPENDIX A
CALCULATION OF THE RECEIVED VIDEO SIGNAL STRENGTH OF TVI SYSTEMS

The object of the following calculation is to determine the number of electrons per picture resolution element resulting from the receiver photomultiplier current (i.e. the received signal) as a function of the laser output power (i.e. the input to the water) and other variables of the system and potential environments. Important system variables include: raster size, raster scan rate, effective diameter of the receiver and the photocathode efficiency of the detector. Important environmental variables include the basic optical properties of ocean waters, the laser scanner-to-target distance and the target-to-receiver distance. In the following, a general calculation is first given and then appropriate values for variables are inserted to generate typical performance curves for the TVI system.

Let P_1 = laser power (CW) [watts]

$\alpha(\lambda)$ = volume attenuation coef. [m^{-1}]

r_1 = laser scanner-to-target distance [meters]

then the incident power on a target at distance r_1 from the laser scanner is given by

$$P_t = P_1 e^{-\alpha r_1} \tag{A-1}$$

If the target has a reflectance $\rho(\theta_i,\theta_e)$, the radiant intensity of the illuminated target element will be

$$J_t = \frac{\rho(\theta_i, \theta_e)}{\pi} P_t \tag{A-2}$$

where θ_i and θ_e are the angles between the normal to the target and the scanner and receiver respectively. For a path between the target and the receiver, distance r_2 [meters], the irradiance at the receiver is given by (Duntley, 1963 Eq. (3-6)).

$$H_R = H_R^o + H_R^\cdot \text{ [watts/m}^2\text{]}, \tag{A-3}$$

where H_R^o is the monopath or unscattered component and is given by

$$H_R^o = \frac{J_t}{R_2^2} e^{-\alpha r_2} \tag{A-4}$$

and $H_R^\cdot$ is the multipath component due to scattering.

If it is assumed that reflectance from the target is relatively diffuse and that the target-to-receiver distance is several attenuation lengths then $H_R^\cdot$, the multipath component of received irradiance due to scattering, may be approximated as

$$H_R^\cdot \approx \frac{J_t K e^{-K r_2}}{2 \pi r_2} \tag{A-5}$$

Alternative assumptions for reflection characteristics may change numerical values of the above approximation, by at most a factor of 3, but do not appreciately alter the following development. With these assumptions, and combining Eqs. (A-3), (A-4), and (A-5), we obtain an expression for H_R which shows the relative contributions from the two components. Thus

$$H_R = J_t \frac{e^{-\alpha r_2}}{r_2^2}\left[1 + \frac{Kr_2}{2\pi} e^{(\alpha - K)r_2}\right] \tag{A-6}$$

Here the first term represents the monopath component which is the only flux useful in conventional imaging systems. The second term yields the magnitude of the multipath or scattered light component which in the TVI system also contributes useful signal flux.

It is now necessary to consider the characteristics of the receiver unit. Let

D_R = diameter of the receiver [m]
η_R = photocathode efficiency of the detector [amps/watt]
P_R = power collected by the receiver [watts]
i_R = receiver signal current [amps]

then

$$P_R = \frac{\pi D_R^2}{4} H_R \tag{A-7}$$

and

$$i_R = \eta_R \bullet P_R \tag{A-8}$$

Combining Eqs. (A-6), (A-7), and (A-8) gives

$$i_R = \eta_R \bullet \frac{\pi D_R^2}{4} \bullet J_t \bullet \frac{e^{-\alpha r_2}}{r_2^2}\left[1 + \frac{K r_2}{2\pi} e^{(\alpha - K)r_2}\right]$$

and by use of Eqs. (A-1) and (A-2),

$$i_R = P_1 \bullet \eta_R \bullet \rho \bullet \frac{D_R^2}{4} \bullet \frac{e^{-\alpha (r_1 + r_2)}}{r_2^2}\left[1 + \frac{K r_2}{2\pi} e^{(\alpha - K)r_2}\right] \tag{A-9}$$

The receiver signal current (Eq. (A-9)) can be expressed in terms of the number of electrons received per picture element, N, since

$$N = \frac{i_R \, \Delta t}{q}\left[\frac{\#\text{ electrons}}{\text{picture element}}\right] \tag{A-10}$$

where

$q = 1.6 \times 10^{-19}$ coulombs (charge on electron)

Δt = interval of time the laser scanner irradiates each picture element.

Thus, the number of electrons per raster position comprising the receiver photomultiplier current is given by

(A-11)

$$N = P_1 \bullet \rho \bullet \frac{D_R^2}{4} \bullet \frac{\Delta t}{q} \bullet \left\{ \eta_R(\lambda) \bullet \frac{e^{-\alpha(\lambda)(r_1 + r_2)}}{r_2^2} \left[1 + \frac{K(\lambda) r_2}{2\pi} e^{(\alpha(\lambda) - K(\lambda)) r_2} \right] \right\}$$

$$= P_1 \bullet \rho \bullet \frac{D_R^2}{4} \bullet \frac{\Delta t}{q} \bullet f(\lambda), \qquad \text{(A-12)}$$

where $f(\lambda)$ is equal to the term in curly brackets { }.

The significance of the above equation is discussed in section II-D. In order to evaluate this expression it is necessary to choose appropriate parameters and to consider the optical properties of water which are dependent upon wavelength.

Equation (A-11) has been evaluated using the following values for the prototype TVI system parameters:

P_1	= 6 milliwatts
ρ	= 0.1
D_R	= 0.051 meters (2" diam. PMT)
η_R	= 0.036 amp/watt @ 632.8 nm (RCA C31000A PMT)
Δt	= 16μ seconds ($\sim$1 second scan of 256 x 256 array)
r_1	= 1 meter
r_2	= variable

In situ data for spectral values of the total attenuation coefficient,α, and the diffuse attenuation coefficient for irradiance, K, for turbid (silty as opposed to biologically active) waters are sparse. Figure A1 gives data from the Fresnell II cruise obtained by Austin and Smith. Near surface, K(10 m) and α (4 m), values are given as well as α values obtained near the bottom just before entering the sediment. Note that for very turbid waters near the bottom, the spectral shape of α appears to be dominated by an almost spectrally flat scattering coefficient.

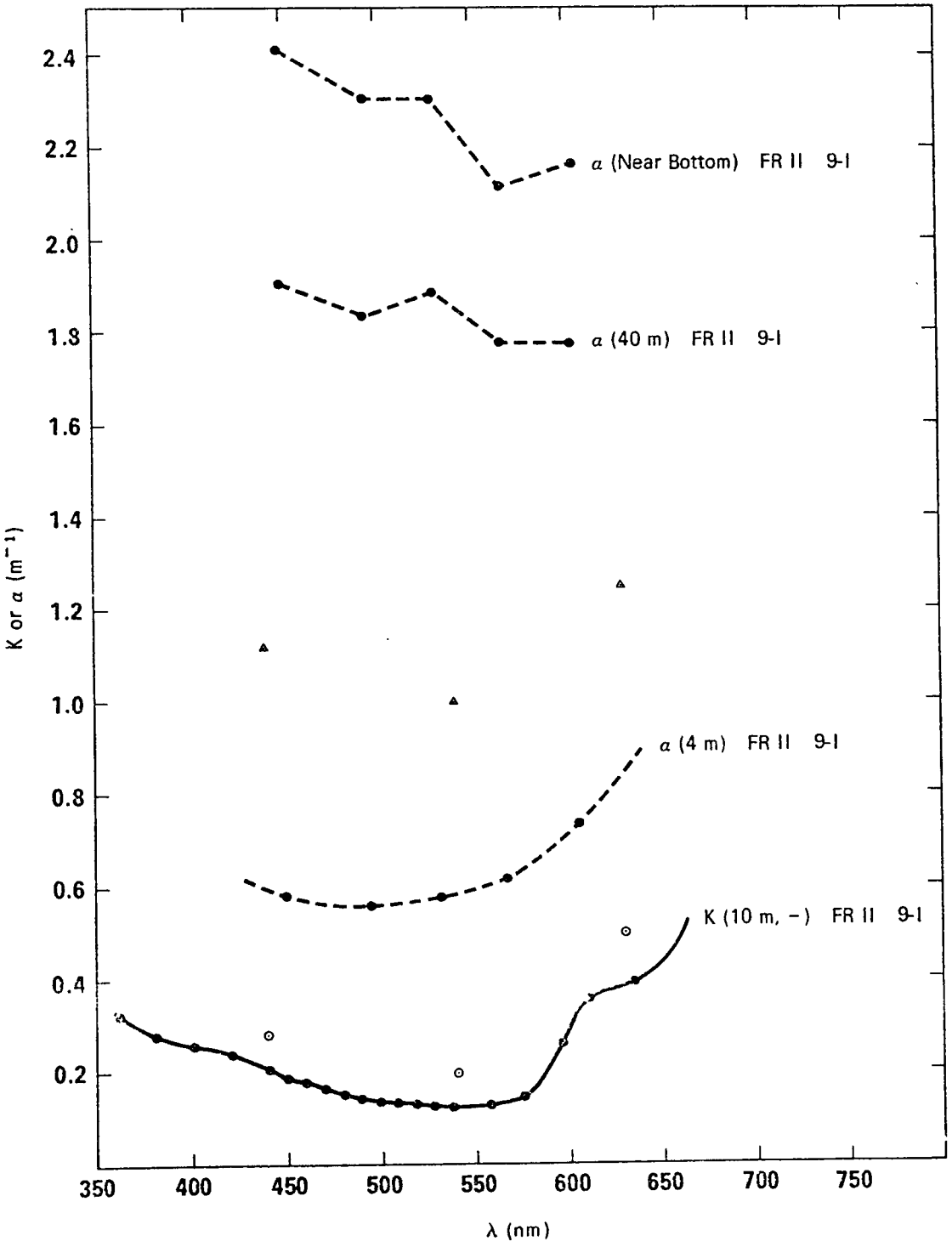
2.4
2.2
2.0
1.8
1.6
1.4
1.2
1.0
0.8
0.6
0.4
0.2
K or α (m⁻¹)
α (Near Bottom) FR II 9-I
α (40 m) FR II 9-I
α (4 m) FR II 9-I
K (10 m, −) FR II 9-I
350
400
450
500
550
600
650
700
750
λ (nm)

FIGURE A1. Turbid water α and K as a function of wavelength. Data from Fresnel II Station No. 9-I (23 March 1971) at north end of Gulf of California. Solid curve shows diffuse attenuation coefficient for irradiance (K (z, λ)), dashed curves show total attenuation coefficient (α (z, λ)). Circles (K) and triangles (α) represent "turbid water model" given in Table A1.

TABLE A1

TURBID WATER MODEL

λ[nm]	440	540	630
α[m^{-1}]	1.120	1.000	1.250
a[m^{-1}]	0.187	0.067	0.317
s[m^{-1}]	0.933	0.933	0.933
K[m^{-1}]	0.280	0.200	0.500

This would imply, for this extremely turbid situation, that all visible wavelengths are equally favorable (or unfavorable) for the TVI system. In fact, this is not likely to ever be true. Since the TVI system is absorption (rather than absorption plus scattering) limited, and absorption at 630 nm is greater than at 540 nm due to the inherent absorption of water, the optimum wavelengths for operation will usually be in the green where absorption is a minimum.

A model for moderately turbid water ($1/\alpha$ = 1 m @ 540 nm) was constructed for calculation purposes following the reasoning used by Tyler *et al.*, (Tyler, Smith and Wilson JOSA 1973) for clear waters. The points chosen for calculation (at λ = 440, 540 and 630 nm) are shown in Fig. A1 and listed (with a and s values) in Table A1.

Using the data from Table A1 and the values listed above Eq. (A-11) was evaluated for various values of target to receiver distance, r_2. The results are shown in Fig. A2. In addition, data from Wilson (Fig. 14 of UCSD thesis, 1973) was used for a separate calculation using the water properties at λ= 630 nm. The solid (Duntley equation) lines refer to a diffuse reflectance target, the dashed (Wilson figure) line to specular reflection. The reflecting characteristics of real objects will lie somewhere between the two.

FIGURE A2. Number of electrons per resolution element (from receiver PMT) for three selected wavelengths using turbid water optical properties given in Table A1 and shown on Fig. A1. Curves calculated using Eq. (A-11). Dashed curve obtained using Fig. 14 of Wilson's thesis (UCSD 1973) for λ = 630 nm and normalized to solid curve at 1 meter. The horizontal scale gives target-to-receiver distance (r_2) and the number of attenuation lengths (αr_2) for red light. The scanner-to-target distance (r_1) was taken to be 1 meter for these calculations.

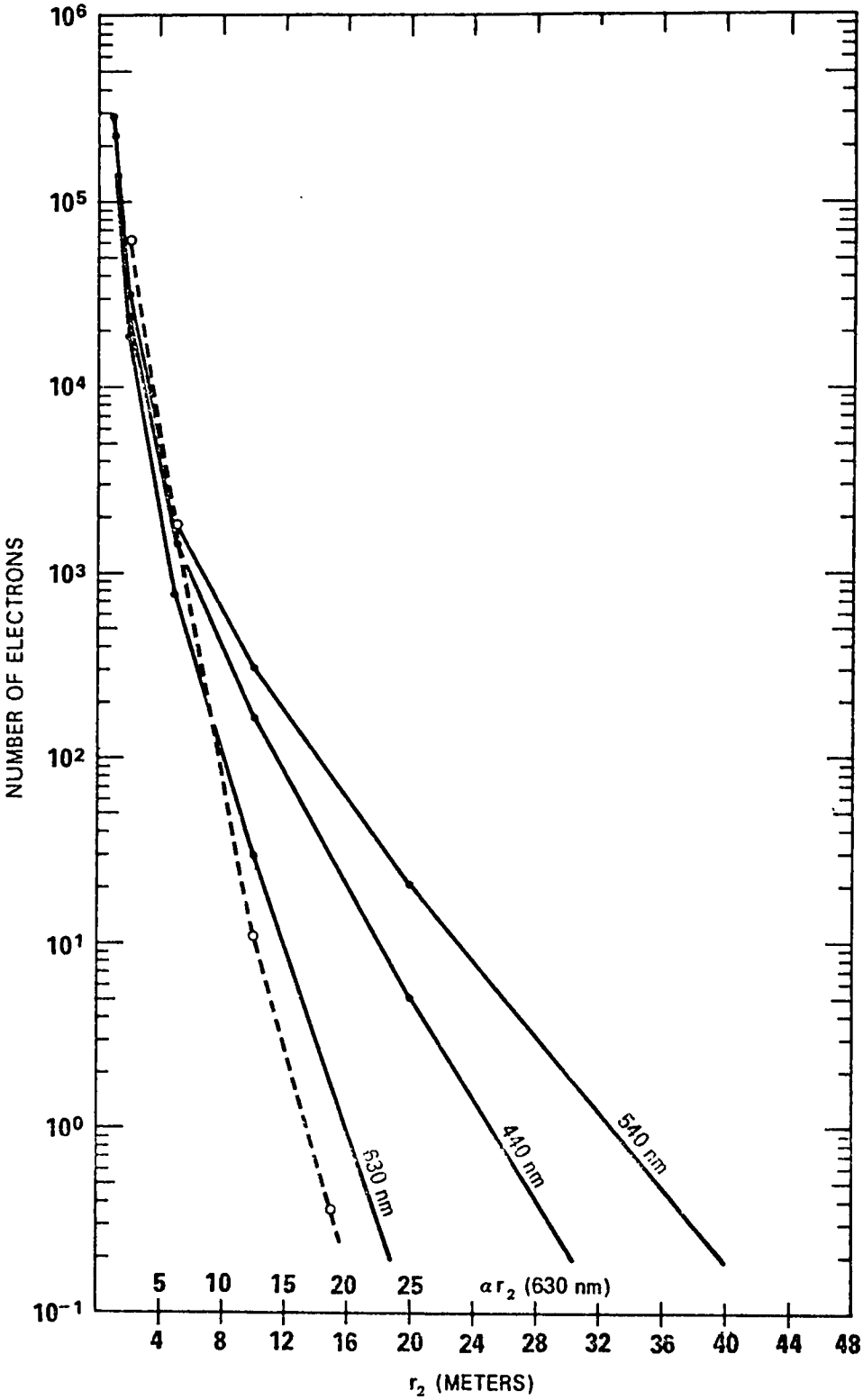
NUMBER OF ELECTRONS
10^6
10^5
10^4
10^3
10^2
10^1
10^0
10^{-1}
630 nm
440 nm
540 nm
5 10 15 20 25 αr_2 (630 nm)
4 8 12 16 20 24 28 32 36 40 44 48
r_2 (METERS)

TVI REPORT APPENDIX B

COMPONENT SELECTION AND TESTS

Laser

A HeNe laser was selected for the initial TVI system in spite of the fact that its output wavelength in the red region of the spectrum is not optimum for transmission through water. It is clear from Fig. A2 that a wavelength in the green region of the spectrum would be an optimum (wavelength) choice for a TVI system. On the other hand, the calculations in Appendix A indicate and previous trials demonstrated, that a TVI system can operate out to some 15 attenuation lengths using red flux. Thus, compact size and proven laser reliability were given priority over an optimum choice of wavelength for transmission. This allowed the prime objectives, an engineering analysis and demonstration of the TVI principle in a diver operated system, to be attained quickly and economically.

At the present time HeNe lasers are the only suitable lasers which are routinely operated by DC batteries and which are mechanically designed and tested to withstand heat, cold, humidity, pressure, vibration and shock. The laser selected for the TVI experimental system has integral mirrors (no cleaning or adjustment necessary), has a hermetically sealed water-resistant head, is environmentally tested and appears to be reliable and durable. The operation of other types of lasers, while offering more power output and a more optimum output wavelength, for portable field use would have required a disproportionate increase in battery capacity, greater initial equipment costs and considerably more engineering effort to achieve the reliability of the present HeNe lasers.

Other considerations remaining equal it is desirable to maximize the output power (P_1 in Eq. (A-11)) from the laser. A study of the HeNe lasers indicated that a transition occurs in commercially available lasers between 5 and 10 milliwatts. Laser units less than 5-10 milliwatts are ruggedly constructed, small in size and power requirements and cost in the neighborhood of $100 per milliwatt (spring, 1974). Above 5-10 milliwatts the cost per milliwatt more than doubles, the overall laser efficiency drops and, thus, the input power requirements rise disproportionately to the output power. Above 10 milliwatts the advantages of HeNe lasers, over those at other wavelengths, begin to diminish.

Table B1 shows a comparison of various commercially available lasers for prospective use in a TVI system with the HeNe system chosen. "Cost" refers only to the off-the-shelf price of the components listed. It is expected that the higher powered systems, especially those requiring liquid cooling of the laser head, would entail higher engineering and development costs which are not included in the table. It has also been assumed that laser AC power supplies can be replaced by DC power supplies without an increase in volume, weight or cost. The comparative figures of merit (volume, weight and cost per power output) make the high power systems appealing but this is somewhat illusory when the total volume and weight are considered (with respect to ease of handling underwater). However, the other figure of merit, $r_{2_{max}}$ (and $\alpha r_{2_{max}}$), makes the high power systems especially appealing, particularly when compared to conventional imaging systems.

TABLE B1

	Present System	General Photonics Model TWO-22 [3]	Hughes Model 3066 [3,6]	Spectra Physics Model 185 [3]
LASER	HeNe	Frequency Doubled ND:YAG	CW ARGON ION	HeCd
Wavelength [nm]	632.8	532	488.0, 514.5	441.6
Beam Diameter @ $1/e^2$ [mm]	0.7	1.2	1.25	1.5
Beam Divergence [mr]	1.15	2.0	<0.65	0.5
Power Output [mw]	6	25	350	50
Power Input [w]	30	550 + 200[2]	4160 + 600[2]	1200
Overall Efficiency [%]	0.02	0.0033	0.007	0.0042
Volume [in^3]	38.7	173	461	4286
Weight [lbs]	1.32	6.6	30	90
Cost[1] [$]	595	6,250[4]	3,790	4,900[7]
LASER POWER SUPPLY	Crestonic			
Normal DC Operation?	Yes	DC/Available [5]	No [5]	No [5]
Volume [in^3]	12.9	114	2128	∿3000
Weight [lbs]	<1	4.4	50	∿50
Cost[1] [$]	238	[4]	2,195	[7]
BATTERIES REQUIRED [10]	8 BD3/10	24 YS-35	16 HR-200	16 HR-70
Voltage [v] - Power [w]	24.8 - 80	25.9 - 840	23.5 - 4700	23.5 - 1624
Volume [m^3] (includes terminals)	127.2	670	1309	514
Weight [lbs]	9.6	49.5	105	40
Cost[1] [$]	607	1440	3132	1495
TOTAL				
Volume [in^3]	179	957	3898 (2.3 ft^3)	7800 (4.5 ft^3)
Weight [lbs]	12	61	195	180
Cost[1] [$]	1440	7690	9117	6395

TABLE B1 (Continued)

	Present System	General Photonics Model TWO-22 [3]	Hughes Model 3066 [3,6]	Spectra Physics Model 185 [3]
$\frac{\text{Volume}}{\text{Power Output}}\left[\frac{\text{in}^3}{\text{mw}}\right]$	29.8	38.3	11.1	156
$\frac{\text{Weight}}{\text{Power Output}}\left[\frac{\text{lbs}}{\text{mw}}\right]$	2.0	2.4	0.56	3.6
$\frac{\text{Cost}}{\text{Power Output}}\left[\frac{\$}{\text{mw}}\right]$	240	308	26[9]	128
$r_{2_{max}}$ [meters]				
(for 10 electrons at receiver in turbid water)	12	34	40	28
$\alpha\, r_{2_{max}}$	15	34	42	31

(1) Prices given for spring 1974.

(2) Estimated power required for cooling pump.

(3) A specific model has been chosen as an example of this class of laser -- other manufacturers models are roughly equivalent.

(4) Price of laser plus DC controller.

(5) Estimate assumes that the laser can be powered by a DC power supply of equivalent volume, weight and cost.

(6) Similar to Hughes model 3057H which the Visibility Laboratory has obtained on loan.

(7) Price includes Model 285 exciter.

(8) Estimated from Fig. A2 assuming parameters similar to present system but optimizing parameters contained in $f(\lambda)$ (Eq. A-12).

(9) Rough estimate taking $\lambda = 500$ nm.

(10) For approximately 1 hour continuous operation.

Battery

Silver-Cadmium batteries were chosen to power the underwater laser scanner unit. Both silver-zinc and silver-cadmium batteries have approximately twice the energy density of nickel-cadmium batteries thus halving the required battery pack space for a given energy output. Equally important, the output voltage as a function of discharge is relatively constant for the silver batteries as compared to nickel-cadmium. While silver-zinc batteries have a somewhat higher energy density than silver-cadmium batteries they cannot be recharged for as many cycles. For these reasons the silver-cadmium batteries were selected.

Figure B1 shows a series of discharge tests run on the laser scanner battery pack. The tests were run at 5 and 10 amp (nominal) discharge rate and at 20°C and at 2°C. The batteries performed to within 50 to 75 percent of their nominally advertised ampere-hour rate. The tests indicate that the batteries operate 10 to 20 percent better at the higher temperature. For this reason the battery packs on the prototype TVI system are insulated. The tests also indicate that the battery packs will be capable of powering the underwater laser scanner unit for one to two hours of continuous operation on a single discharge cycle.

Sychronization Lamps

A series of light-emitting diodes (LED's) and a Xenon flashtube were tested and evaluated as sources for the TVI sync pulse. The LED's have the advantage of very small size and low power consumption.

FIGURE B1. Battery pack output voltage vs time for several discharge rates and operating temperatures. Curves 1, 3 and 5 show test results at a discharge rate of approximately 5 amps while curves 2 and 4 show results for a discharge rate of 10 amps. Curves 1, 2 and 5 show test results while operating the batteries at room temperature (∿20°C) while curves 3 and 4 show test results while operating the batteries at 2°C. V_{min} and V_{max} note the voltage range of the underwater electronics. A 1% voltage change is also noted.

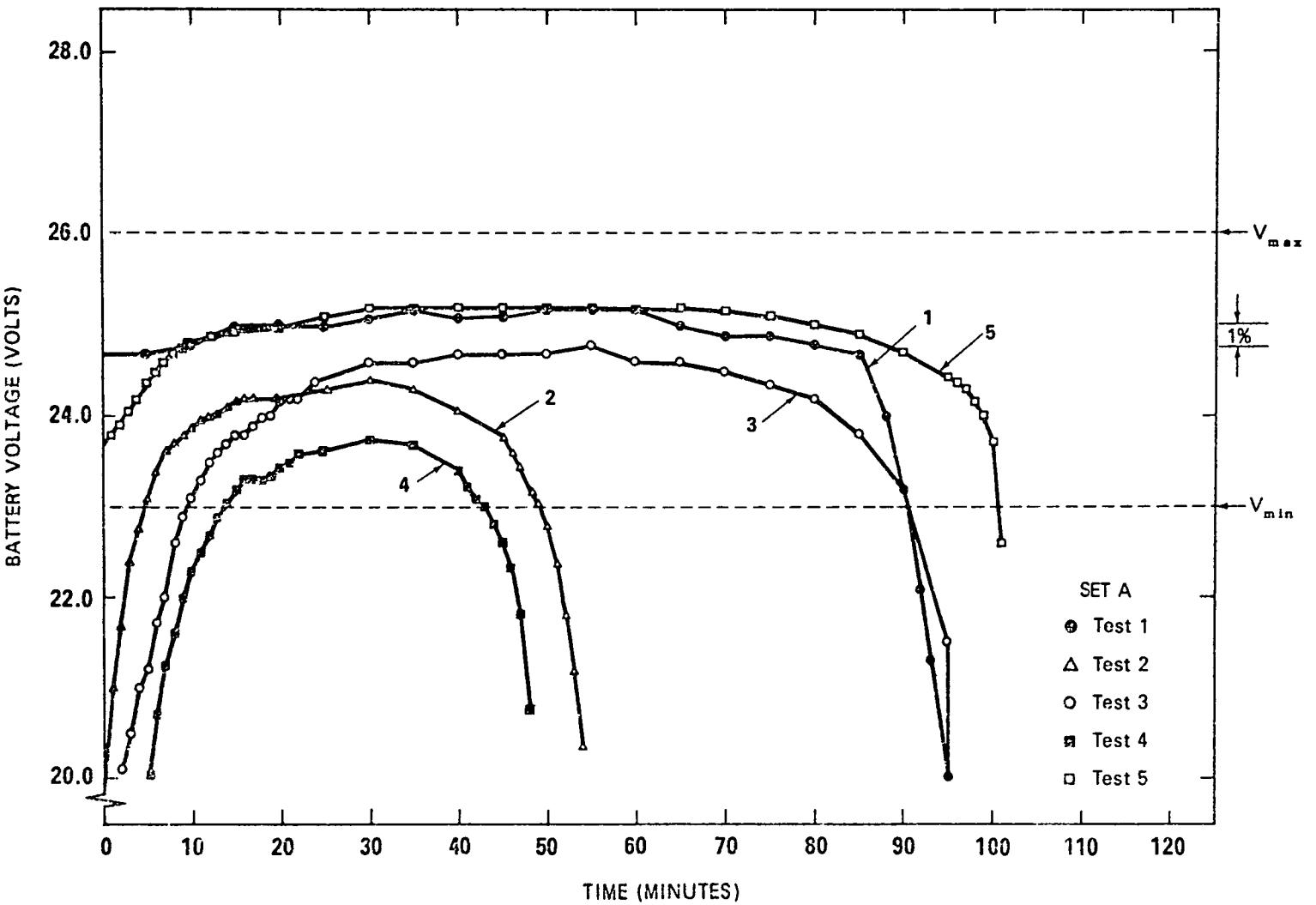
28.0
26.0
24.0
22.0
20.0
BATTERY VOLTAGE (VOLTS)
0
10
20
30
40
50
60
70
80
90
100
110
120
TIME (MINUTES)
V_{max}
V_{min}
1%
1
2
3
4
5
SET A
Test 1
Test 2
Test 3
Test 4
Test 5

However, the output power of the LED's tested was not adequate to provide a reliable sync pulse through many attenuation lengths of water. The Xenon flashtube is somewhat larger in size and power consumption but the tested model has a power output (within the spectral range of a Kodak Wratten No. 44 filter) more than 3000 times that of the LED's tested.

A EG&G Model #FX-101 Xenon flashtube (filtered with a Kodak Wratten No. 44 filter) and a photomultiplier receiver were placed at opposite ends of the Visibility Laboratory's 13 meter test tank. The absorption and scattering coefficient of the water between the flashtube and receiver was systematically increased while measurements of the optical water properties and the characteristics of the received sync pulse were made. Results of this test are shown in Fig. B2 which plots relative photomultiplier tube voltage versus the total attenuation coefficient of the water. The last point (dotted portion of the curve) was extrapolated from the known remaining gain factor of the photomultiplier. This test demonstrated that a 1 volt signal pulse (more than suitable to initiate synchronization) could be transmitted through 12.7 meters of $\alpha = 3.12$ meter water, i.e. through 39.6 attenuation lengths.

Thus, by utilizing two Xenon flashtubes, situated on each side of the prototype TVI system, we assure that the maximum operational range of the system will not be limited by the sync pulse. This is particularly important for the testing and evaluation of the TVI system.

FIGURE B2. Relative photomultiplier tube signal voltage (from EG&G Model No. FX-101 Xenon flashtube filtered with a Kodak Wratten No. 44 filter and passed through 12.7 meters of water) versus the total attenuation coefficient of the water. The last data point (dashed portion of the curve) was extrapolated from the known remaining gain factor of the photomultiplier. The wide range of relative voltages is due to renormalizations from gain factors and neutral density filters used.

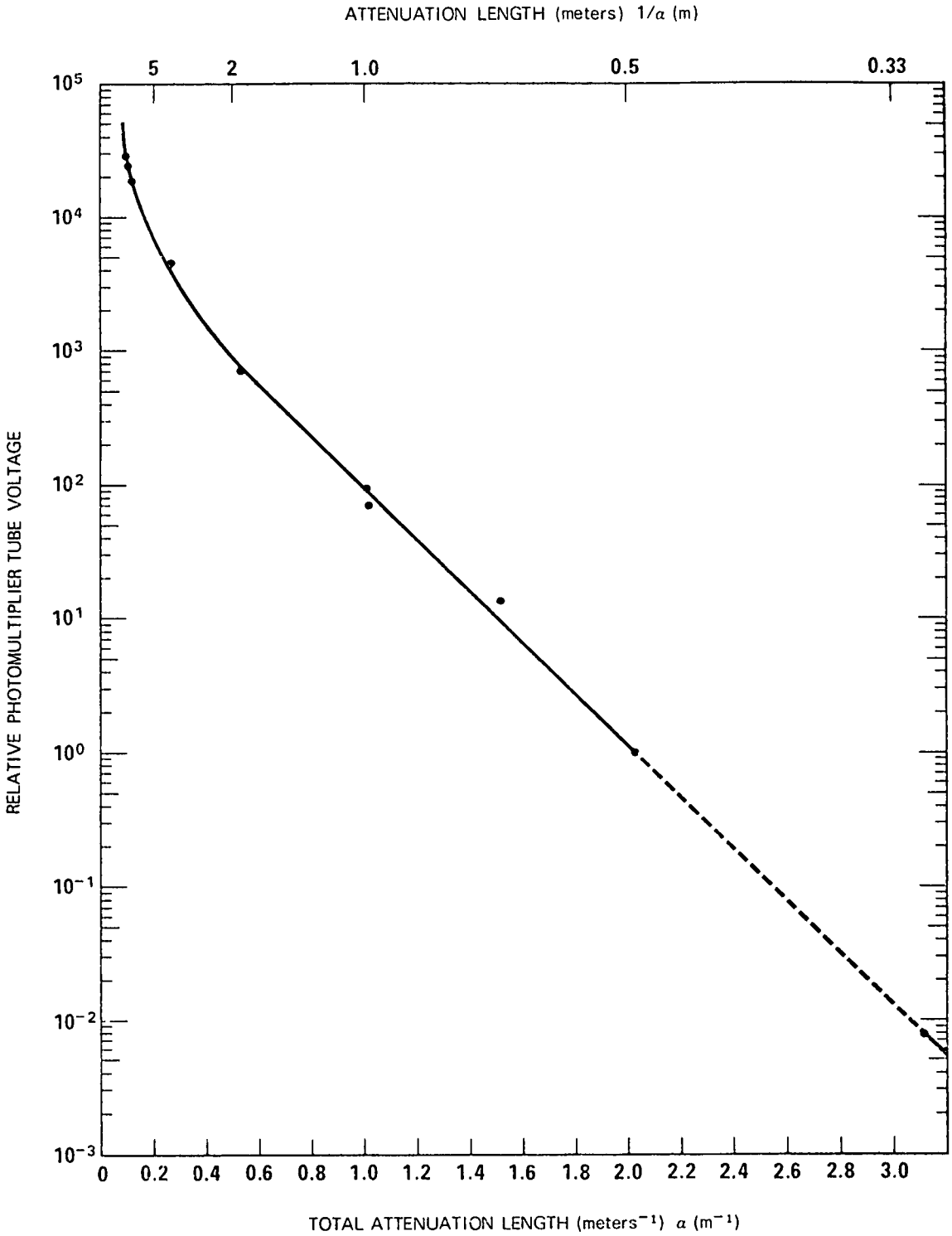
ATTENUATION LENGTH (meters) 1/α (m)
5
2
1.0
0.5
0.33
RELATIVE PHOTOMULTIPLIER TUBE VOLTAGE
10^5
10^4
10^3
10^2
10^1
10^0
10^-1
10^-2
10^-3
0
0.2
0.4
0.6
0.8
1.0
1.2
1.4
1.6
1.8
2.0
2.2
2.4
2.6
2.8
3.0
TOTAL ATTENUATION LENGTH (meters^-1) α (m^-1)

Receiver Filter

As described in the text, an RCA C31000A photomultiplier is used to detect the time encoded laser signal reflected from the target. It is desirable that this receiver have a wide field of view and to be sensitive to only wavelengths emitted by the laser. To restrict the received signal to wavelengths in the vicinity of laser wavelength an interference filter is used in front of the TVI receiver photocathode. However, use of an interference filter narrows the receiver field of view. Studies were made in order to obtain an optimum wide field of view while at the same time restricting the receiver to a narrow spectral band.

When light passes through an interference filter at angles other than normal to the filter, a shift in the transmitted passband wavelength and a loss in transmission occurs. Both of these effects are a function of the angle of incidence. Studies were made to see if the use of additional optical lenses could be used to increase the field of view while at the same time limiting the angles of incidence of light passing through the interference filter. It was found that the potential gain in receiver sensitivity did not warrant, at least for the present system, the required increase in size, complexity and cost. Consequently, it was decided to utilize only an interference filter in front of the receiver photomultiplier with no accessory optics.

The laser light is effectively blocked by the interference filter beyond certain angular limits due to the shift, toward the shorter wavelengths, of the bandpass of the filter with increasing angle. Because of this shift it is possible to increase the effective receiver field of view by choosing the center wavelength of the interference filter to be slightly larger (636.2 nm) than the laser wavelength (632.8 nm). In this way, as the angle of incident light increases, the center of wavelength acceptance moves toward and then past the laser wavelength resulting in a wider acceptance angle with a small cusp at normal incidence. Calculations indicated that an interference filter with a nominal center wavelength of 632.3 nm with a half bandwidth of 11.2 nm would be an optimum choice.

After procurement of a Ditric three cavity interference filter its spectral transmission was measured using a Cary 14 Spectrophotometer. This filter was found to have a center wavelength of 632.7 nm, a half bandwidth of 11.0 nm and a peak transmission of 59%. The measured relative filter transmittance versus incident angle for laser light at 632.8 nm is shown as the solid curve in Fig. B3. The relative transmittance versus incident angle, for diffuse ambient light uniformly distributed with wavelength, is shown as the dashed curve. The latter curve is determined from the measured relative spectral bandpass for several angles of incidence as shown in Fig. B4. The integrated area under each passband, for a given angle of incidence, gives the relative response at that angle (as plotted in Fig. B3).

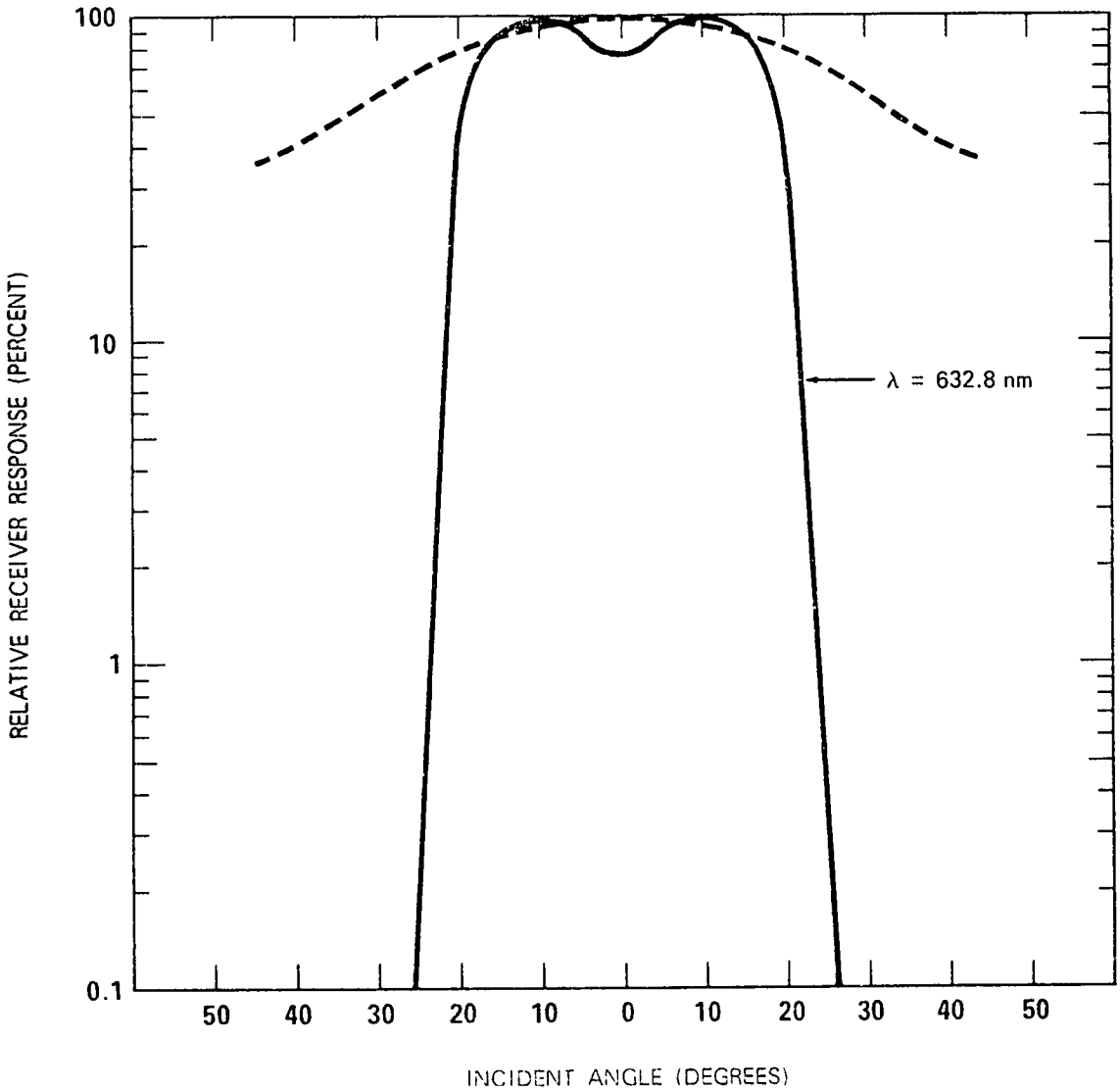

FIGURE B3. Relative transmittance versus angle of incidence for video receiver interference filter (ditric three cavity interference filter). The measured relative filter transmittance for laser light at 632.8 nm is shown as the solid curve. The dashed curve shows the relative transmittance for diffuse ambient light uniformly distributed with wavelength.

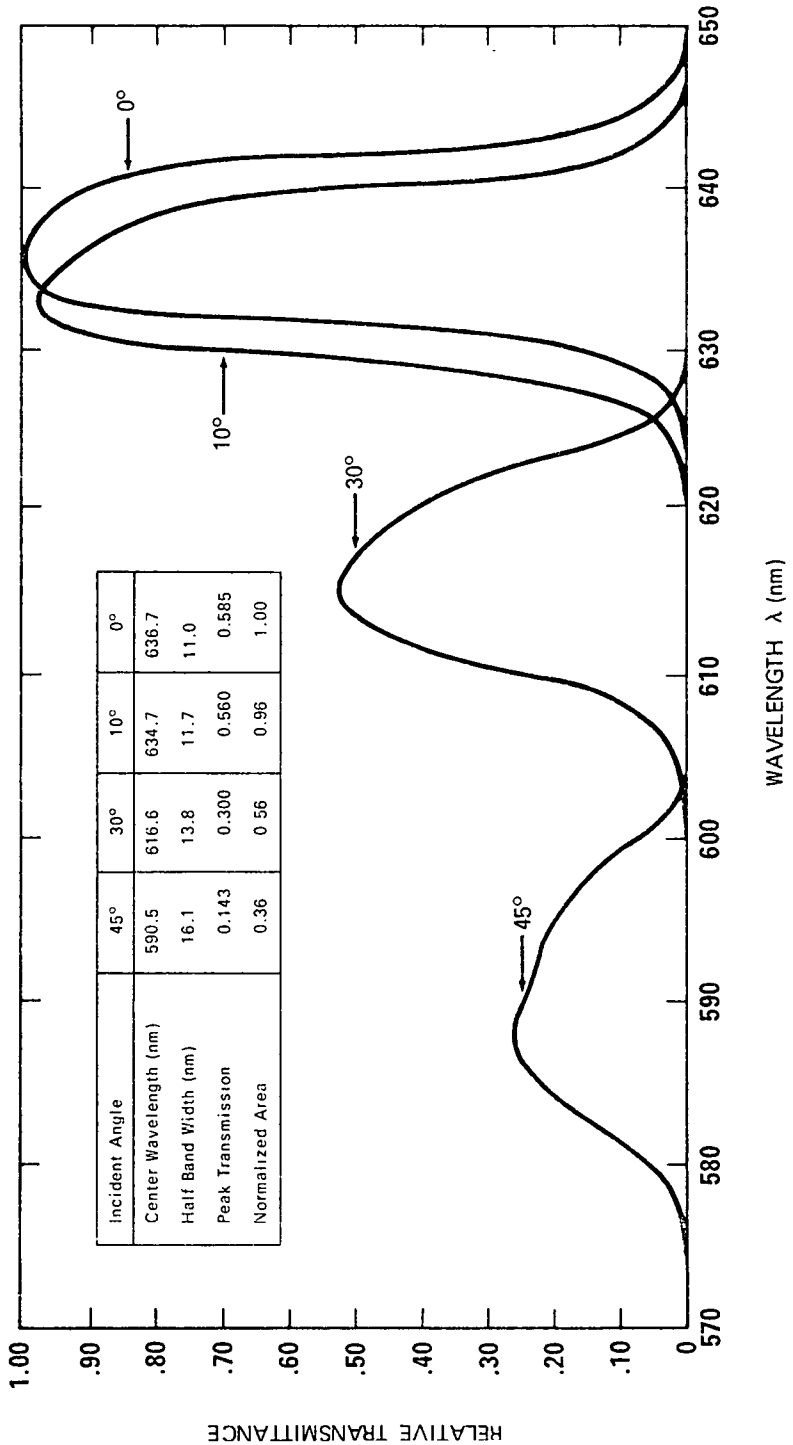

FIGURE B4. Measured relative spectral bandpass (for receiver interference filter) as a function of wavelength for several angles of incidence. The table inserted on the graph gives, for each angle of incidence, the center wavelength of the passband, the half bandwidth, the peak transmission and the normalized area under the passband curve. The normalized area gives the relative transmittance for diffuse ambient light uniformly distributed with wavelength and provides the data for the dashed curve in Fig. B3.

PREFACE TO PART II

Part I of this report described in detail the Basic Principles (§II A), System Components and Specifications (§II B and C) and Design Considerations (§II D) for an experimental TVI system. Also discussed in Part I were previous experimental trials using a breadboard TVI system and tests of the selected components.

An engineering model of the TVI system was completed in early July. Part II of this report will discuss preliminary tests and evaluation of this experimental model performed during July and August 1974. This includes laboratory-bench tests, laboratory-tank tests and tests performed by divers underwater in very turbid San Diego Harbor water.

Part I contained Sections I an II, Appendices A and B, Figures 1 through 13, A1, A2, B1 through B4, and Tables A1 and B1. Part II contains Section III and IV and Figures 14 through 28.

Table of Contents
Part II

Table of Figures
Part II

III. EXPERIMENTAL TVI SYSTEM, PRELIMINARY TEST AND EVALUATION

A. Bench Tests

FIGURES 14 and 15 show photographs of the underwater laser scanner unit in its underwater housing. Figure 14 should be compared to Figure 3 which shows the laser-scanner unit without the underwater housing. As described previously, the underwater unit is self-contained and may be operated by a diver unencumbered with an umbilical associated with the equipment. Alternatively, for some test and evaluation purposes, the underwater laser scanner may be operated remotely by means of an umbilical cable.

Laboratory-bench tests were concerned primarily with checking out and adjustment of the TVI system. All electronic components were checked for proper performance, mechanical and optical components were aligned and the scan size and range adjustments set. All modes of operation described in Section II C 3 were tested with the laser scanner in air and all necessary adjustments to the system were made.

B. Tank Tests

The routine system check-out described above was repeated with the instrument in the Visibility Laboratory's 13-meter test tank. First, all modes of operation (§II C 3) were again checked out and final electronic and optical adjustments made. Second, the performance of the system was tested under laboratory conditions by systematically adjusting the optical properties of the tank water. Figures 16 through 20 show a selection of test results using the experimental TVI system in the test tank. It should be recalled that the underwater laser scanner in this experimental system utilizes a 6 milliwatt HeNe laser (§II B and Appendix B) emitting at 632.8 nm.

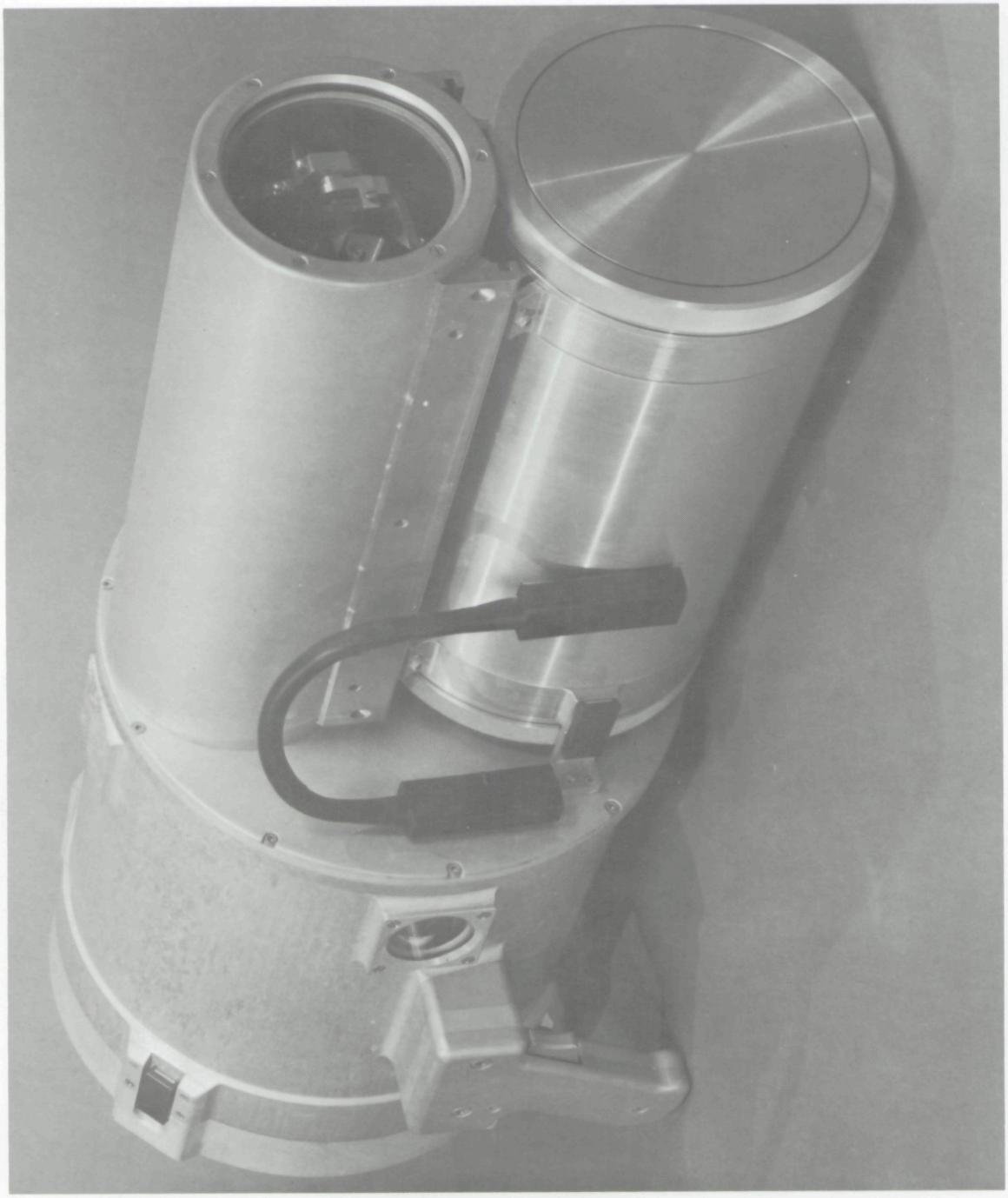

FIGURE 14. Photograph of underwater laser scanner unit in its underwater housing (compare with Figure 3). The laser beam exits through a 3/8" thick acryllic window. Below the laser housing is the larger diameter battery housing, which may be easily removed from the remainder of the underwater housing. A short cable, with underwater connectors, connects the underwater battery pack to the underwater housing. The exit port for the sync pulse flash lamp (one of two) can be seen on the side of the underwater housing. The underwater unit is carried by means of either or both of two handles. The handle which can be seen in the photograph contains the hand trigger for initiating a scan sequence.

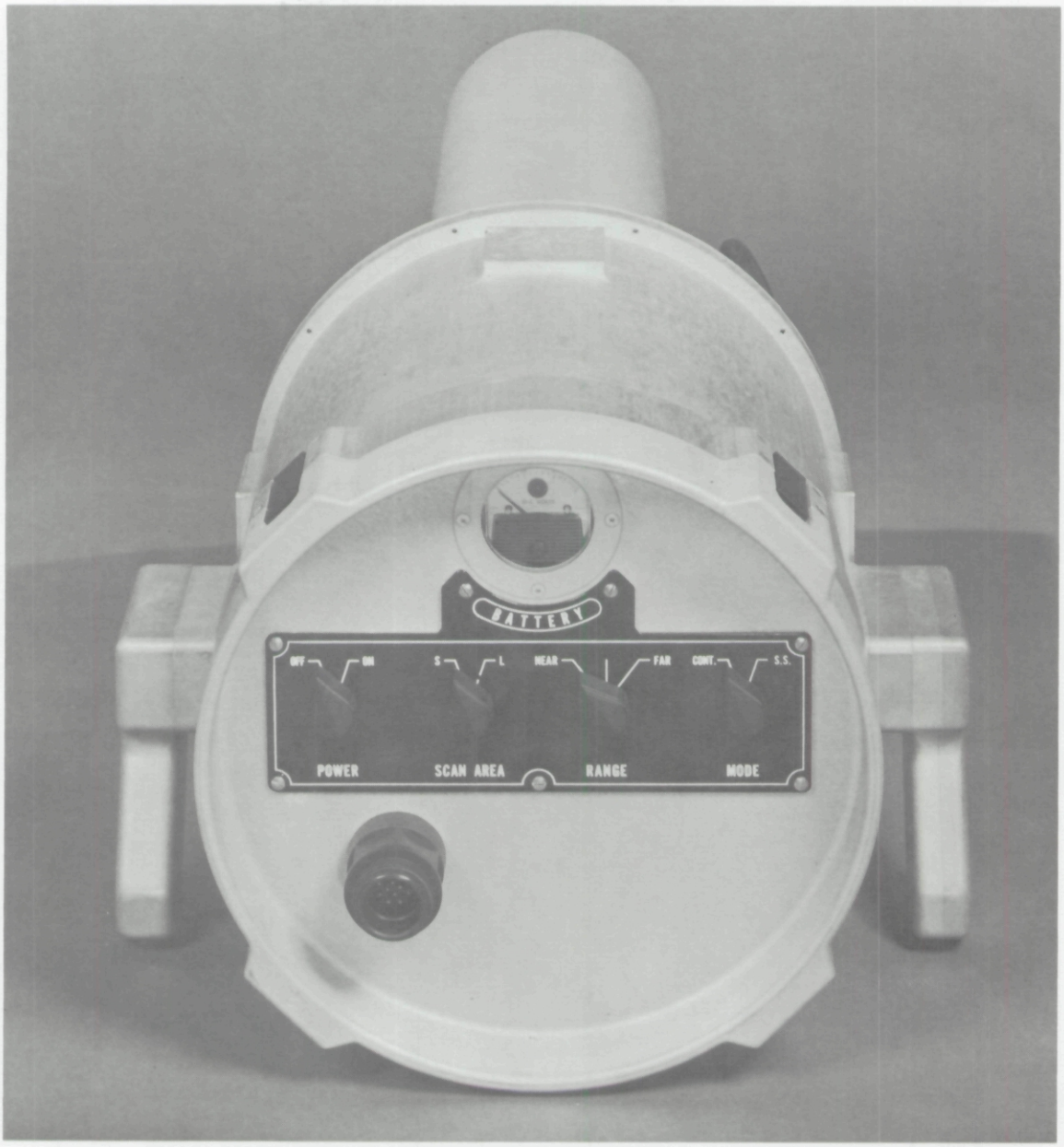

FIGURE 15. Photograph of underwater laser scanner unit in its underwater housing from a diver's perspective. This view shows the two handles (the right handle containing the hand trigger for initiating a scan sequence) and the underwater control panel. The control panel includes: a DC voltmeter to indicate battery voltage; a power on-off switch; a switch to select a wide (∿18°) or narrow (∿5°) angular field of view for the underwater scan; a range adjustment for optimizing laser beam spot size; and a mode selection switch for continuous or single-shot scanning. These controls have been designed for ease of operation by a diver underwater, but they are primarily for test and evaluation purposes. Routinely, a diver need only to turn the power on, aim the laser scanner and pull the pistol-grip trigger to initiate an imaging sequence. The control panel also contains an underwater connection for an umbilical cable which provides the alternative of remote operation of the underwater unit.

Figure 16 shows two Polaroid photographs of TVI images of a navy resolution chart. Image (a), taken at 1 meter with a scan angle of 12°, shows the entire chart. Image (b), taken at a laser scanner-to-target distance of 0.25 meters with a scan angle of 3°, resolves the smallest bars in the center of the chart. This represents a resolution of 4.5 line pairs per millimeter in object space.

As described in Part I, the resolution for wider scan-angle images (as in Figure 16a) is limited by the number of resolution elements in the array. This is because the angular distance between picture elements of the array is larger than the angular beam spot size of the laser, and thus the distance between picture elements determines the resolution. Conversely, resolution for the narrower scan-angle images (as in Figure 16b) is limited by the laser beam spot size, since angular spot size is larger than the angular distance between picture elements. In this case the size (diameter plus divergence) of the laser beam determines the resolution.

In addition to quantitatively demonstrating the resolution capability of the experimental TVI system, Figure 16 shows the effect of varying the scanning angle. The effect of decreasing TVI scan angles is much the same as increasing the focal length of a zoom lens in a conventional system.

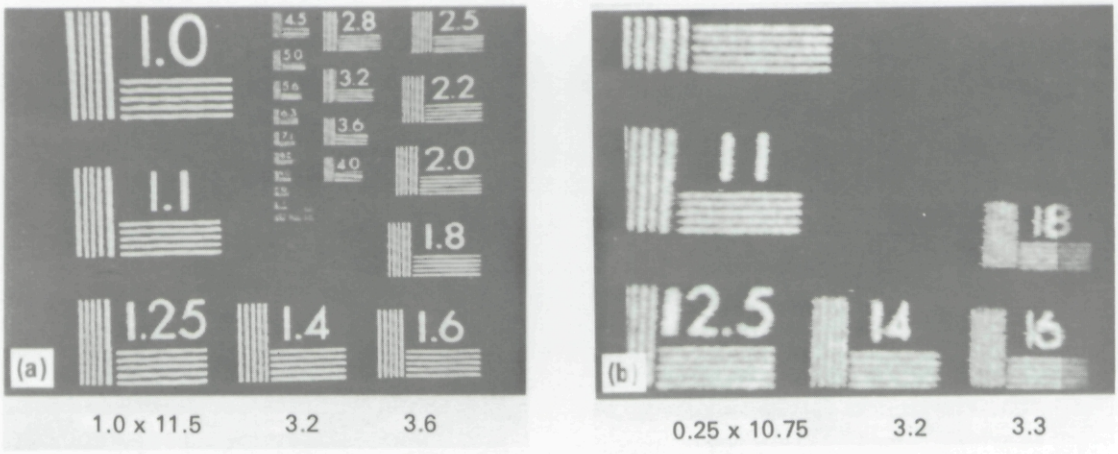

FIGURE 16. Images obtained using the experimental TVI system in the Visibility Laboratory 13 meter test tank. In this, and the following four figures (which are photographs of photographs of oscilloscope displays), the captions below individual images give: the laser scanner-to-target distance (r_1) and the target-to-receiver distance (r_2), in meters; the attenuation length ($1/\alpha$) of the water, in meters; the total number of attenuation lengths (αr_2) over which the image has been propagated. The experimental TVI system utilized a 6 millivolt red (632.8 nm) laser and a 256 x 256 array size scanned in 1 second for all the figures shown below.

This figure shows two images of a navy resolution chart. The chart consists of horizontal and vertical bars of equal widths and spaces. The width of a bar (or space) in millimeters is equal to 2/n where n is the numeral associated with each group of bars. Image (a), taken at 1 meter with a scan angle of 12°, shows the entire chart. Image (b), taken at a distance of 0.25 meters with a scan angle of 3°, resolves the smallest bars in the center of the chart. This represents a resolution of 4.5 line pairs per millimeter in object space.

Figure 17 presents less quantitative but more graphic examples of the resolution capability of the experimental TVI system. Images (a) and (b) are of a Roosevelt dime, an object that provides relatively low contrast. The images were obtained in clear water with a 3° scan angle. The first image was at a distance of 0.33 meters (12 inches). The word "liberty," composed of 1.3mm (∿ 1/16 inch) letters, can be easily read. In image (b), obtained at a laser scanner-to-target distance of 0.18 meters (7 inches), the words "In God We Trust" can be read along with the information that it is a 1970 dime from the Denver mint. These letters are about 0.8mm (0.03 inch) high.

Image (c), an auto-club membership card providing relatively high contrast, was scanned at a distance of 1.5 meters using a scan angle of 3°. The member's name, the name of the club, and the numerals can be read. The largest lettering in the card is 3.0mm (1/8 inch) high. The member's name is in 2.5mm (3/32 inch) letters. The images shown in Figure 17 graphically demonstrate that the experimental TVI system is capable of producing high-resolution images of both high- and low-contrast objects.

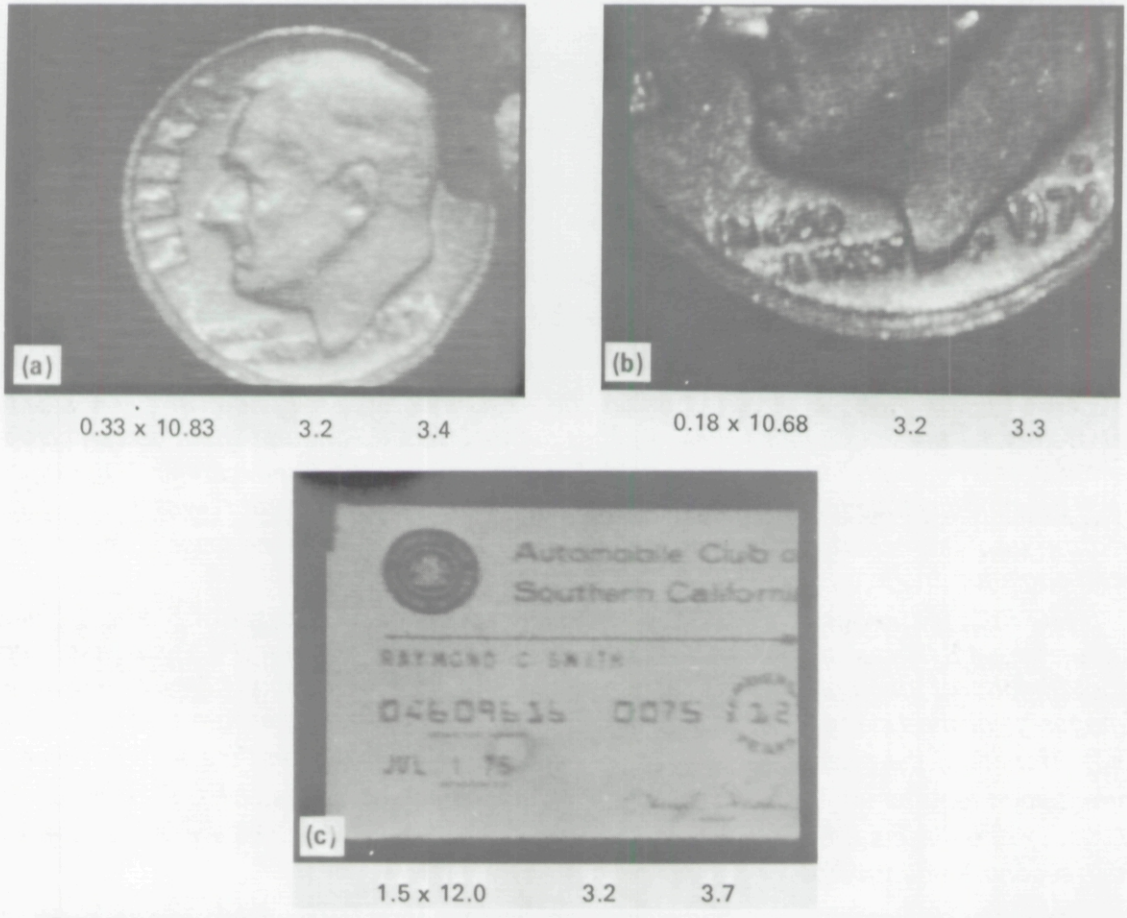

FIGURE 17. Images obtained using the experimental TVI system in the Visibility Laboratory 13 meter test tank. These images demonstrate that the TVI system is capable of producing high resolution images of both high- and low-contrast targets. On the low-contrast dime, the letters in the word "liberty" are about 1.3mm (∿ 1/16 inch) high; the letters in "In God We Trust" are about 0.8mm (∿ 0.03 inch) high. The largest letters on the high-contrast auto-club membership card are 3.0mm (∿ 1/8 inch) high, and the member's name is in 2.5mm (∿ 3/32 inch) letters.

An important advantage of a TVI system over conventional imaging systems is its relatively large depth of field. This is demonstrated by the two images shown in Figure 18. The register counter on the right-hand side of the image was at a laser scanner-to-target distance of 0.5 meters; the counter on the left-hand side was at 1.0 meters; and the resolution chart was at a distance of 1.5 meters. Both images show that good resolution was obtained simultaneously at all three target distances. As discussed in Part I, this is a result of the small diameter and small angular divergence of the laser beam.

Figure 19 shows six images obtained with the experimental TVI system in the laboratory-test tank of the navy resolution chart and a small register counter. The resolution chart was 1.0 meters and the counter 0.5 meters from the laser scanner.

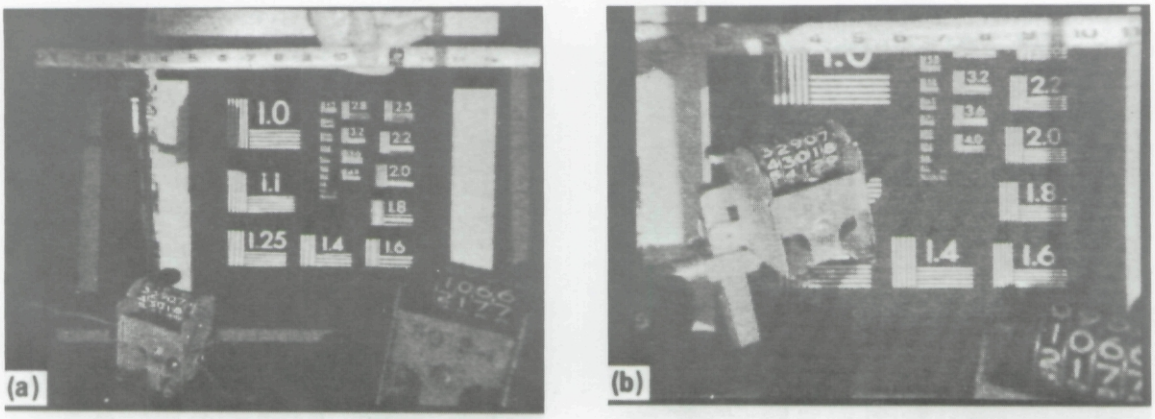

Scan Angle 17°

Scan Angle 11°

FIGURE 18. Images obtained using the experimental TVI system in the Visibility Laboratory 13 meter test tank. These images demonstrate that good resolution can be obtained over a relatively large depth of field. For both images the laser scanner to the right-hand counter distance (r_1) was at 0.5 meters, for the left-hand counter r_1 was 1.0 meters, and the resolution chart and tape measure were 1.5 meters from the laser scanner. The scan angle for image (a) was 17° and for image (b) it was 11°.

The front dimensions of these counters are 4.2 cm (1.65 inches), the sides are 3.8 cm (1.50 inches) and the heights 5.9 cm (2.32 inches). The "zeros" on the counters have an outside diameter of 0.42 cm (0.18 inches).

FIGURE 19. Images obtained using the experimental TVI system in the Visibility Laboratory 13 meter test tank. These images show the increasing degradation in image quality due to decreased signal-to-noise ratio as the attenuation length ($1/\alpha$) of the water is decreased. They also demonstrate that resolution, per se, was not degraded as the number of attenuation lengths between the target and the receiver (αr_2) was increased. The images also show good depth of field and the relative degradation of targets placed at separate target-to-laser scanner distances. Scanning angle for all images was 3°.

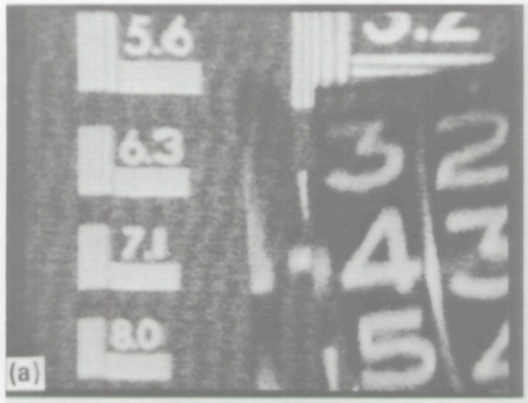

$1/\alpha$ = 3.22 meters αr_2 = 3.42

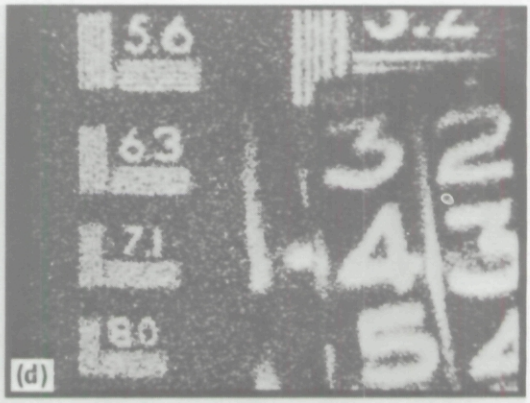

$1/\alpha$ = 0.99 meters αr_2 = 11.12

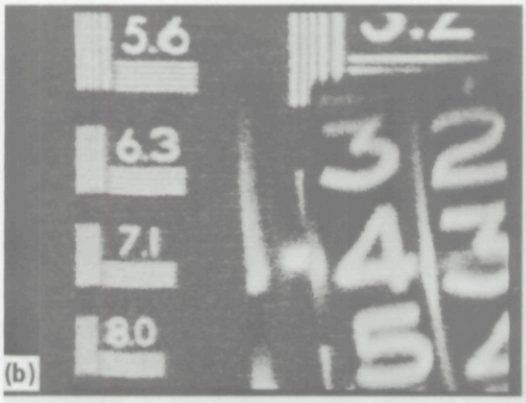

$1/\alpha$ = 1.96 meters αr_2 = 5.61

$1/\alpha$ = 0.785 meters αr_2 = 14.00

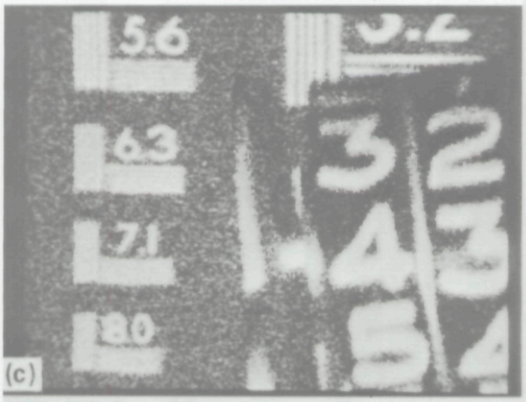

$1/\alpha$ = 1.33 meters αr_2 = 8.26

$1/\alpha$ = 0.66 meters αr_2 = 16.65

Counter 0.5 x 11.0 meters Navy Resolution Chart 1.0 x 11.5 meters

The target scene remained the same while the optical properties of the water in the test tank were varied to provide an increasing number of attenuation lengths for image propagation. The attenuation length ($1/\alpha$) and the total number of attenuation lengths (αr_2) for image propagation are shown below each image. This series of images demonstrates that high-quality images can be obtained through many attenuation lengths of water. A comparison of the images shows the increasing degradation in image quality due to decreased signal-to-noise ratio as the attenuation length ($1/\alpha$) of the water is decreased. Note, as described in Part I, that image resolution, per se, was not degraded as the number of attenuation lengths between the target and the receiver (αr_2) was increased.

Figure 20 shows six images of a diver's watch with the name "ARDATH" on the face. This figure demonstrates that good quality images can be obtained through many attenuation lengths of water using the experimental TVI system. The first five images were obtained using the same scan angle and target-to-receiver distance while varying the attenuation of the water. As in previous figures, it can be seen that the image quality, but not resolution, is degraded as the number of attenuation lengths is increased. Images (a) through (d) are useful images providing fine detail of the diver's watch and even image (e), propagated through 23 attenuation lengths of water, still conveys some image information.

For image (f), the target-to-receiver distance was reduced to 6.25 meters for comparison with image (c). Both images (c) and (f) were propagated through slightly more than 13 attenuation lengths (αr_2) of water but $1/\alpha$ and r_2 for image (f) are roughly half the corresponding values for image (c). The noise evident in image (c) is greater than in image (f), and the quality of the latter is slightly better than that of image (c), even though they traveled the same number of attenuation lengths. This is attributed to the fact that the absorption loss in (c) was greater than in (f). As discussed in Part I, it is absorption, as opposed to scattering, which limits a TVI system. Thus, given the same attenuation length ($1/\alpha$), a TVI image may be propagated further through water with a higher ratio of scattering to absorption than one with a relatively low s/a ratio.

FIGURE 20. Images obtained using the experimental TVI system in the Visibility Laboratory 13 meter test tank. These images show that good quality images can be obtained through many attenuation lengths of water using the experimental TVI system. All images were taken at the same target-to-laser scanner distance of 0.25 meters with a 3° scanning angle. The target-to-receiver distance was 10.75 meters for the first five images (a through e) and the attenuation of the water was varied. For image (f) the target-to-receiver distance was reduced to 6.25 meters for comparison with image (c). See text for details.

The dimensions of this watch are: outside diameter of movable bezel, 1-1/2 inches; diameter of inner lapse-time dials, 5/16 inch; height of numbers on watch face, 1/16 inch; height of numbers on lapse-time dial, 1/32 inch; height of letters in word "ARDATH," 1/32 inch.

$1/\alpha$ = 3.2 meters αr_2 = 3.34

$1/\alpha$ = 0.66 meters αr_2 = 16.2

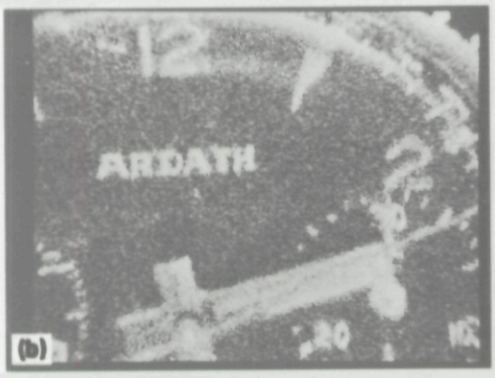

$1/\alpha$ = 0.99 meters αr_2 = 10.9

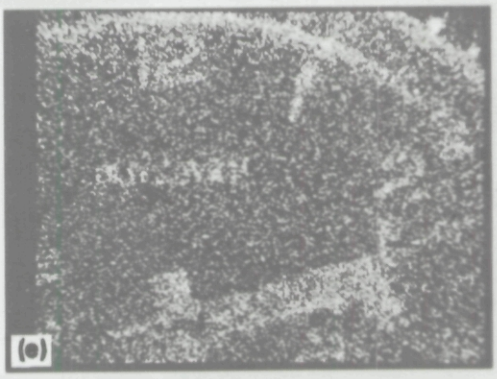

$1/\alpha$ = 0.46 meters αr_2 = 23.1

$1/\alpha$ = 0.79 meters αr_2 = 13.7

0.25 x 10.75

$1/\alpha$ = 0.46 meters αr_2 = 13.4

0.25 x 6.25

While in the test tank the relative response of the TVI receiver was evaluated as a function of the angle of incidence of light coming from the direction of the target. With the Ditric three cavity interference filter (Part I, Appendix B) the measured response was very similar to that shown by the solid curve in Figure B4. The interference filter on the video receiver was then replaced by a Kodak Wratten No. 29 filter and again the relative response vs. the angle of incidence was measured. The results of these measurements are shown in Figure 21. These results indicate that the angular width of the relative response of the video receiver is roughly twice as

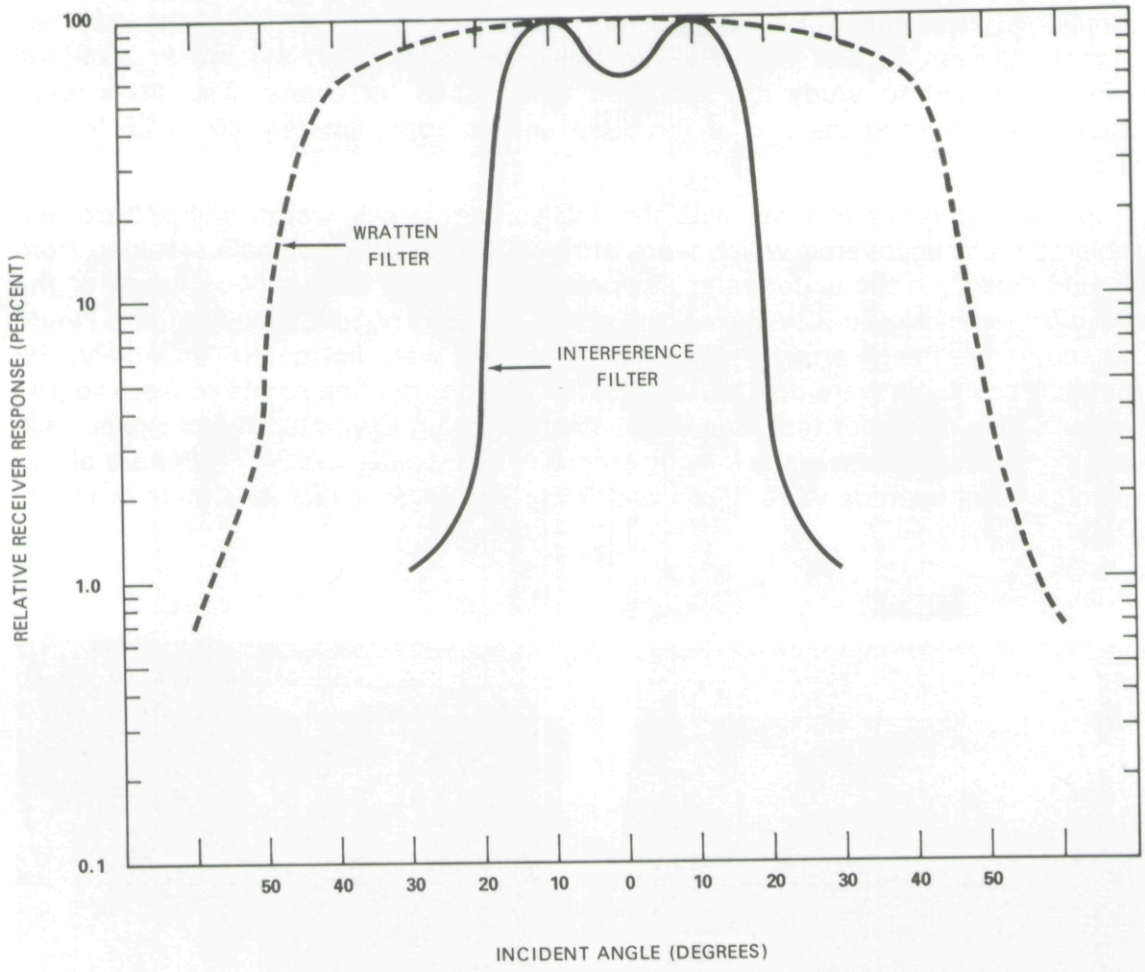

FIGURE 21. Relative receiver response vs. angle of incidence for video receiver with filters. The solid curve is the measured response of the experimental TVI system utilizing a Ditric three cavity interference filter over the video receiver. The dashed curve is the response utilizing a Kodak Wratten No. 29 filter. The tank tests (§III B) were performed utilizing the interference filter while the harbor tests (§III C) were performed utilizing the Wratten filter.

large using the Wratten filter as that obtained with the interference filter. Thus, from the standpoint of geometrical response, the Wratten filter is the best choice for use in the video receiver. However, further tests are necessary to establish which filter provides the best overall rejection of backscattered and/or ambient light. Thus it is not yet certain which filters are the optimum choice for the video receiver. The tank tests discussed above were performed with the interference filter over the video receiver. The harbor tests, discussed below, were performed with the Wratten filter over the video receiver.

C. San Diego Harbor Tests

The final series of tests, during this funding period, were performed using the experimental TVI system in San Diego Harbor. The principal objective of these harbor experiments was to test and evaluate the experimental TVI system in a natural environment and to study its operation when used by divers. The tests were conducted at night at the end of the S.I.O. pier in approximately 20 to 25 feet of water.

In the first series of tests with the TVI system in salt water, image-distortion problems were uncovered which were attributed to small ac signals resulting from "ground loops" in the underwater equipment. Figure 22 shows two images of the resolution chart. Figure 22a shows the effect of the grounding problem and Figure 22b shows the image after all grounding problems were corrected. Unhappily, the grounding problems were only partially corrected after our first series of tests so that the last series of harbor tests were still affected by an unwanted noise signal. This noise signal can be seen in the images shown in Figures 23 and 24. Ultimately all extraneous noise sources were eliminated from the image signal as shown in Figure 22b.

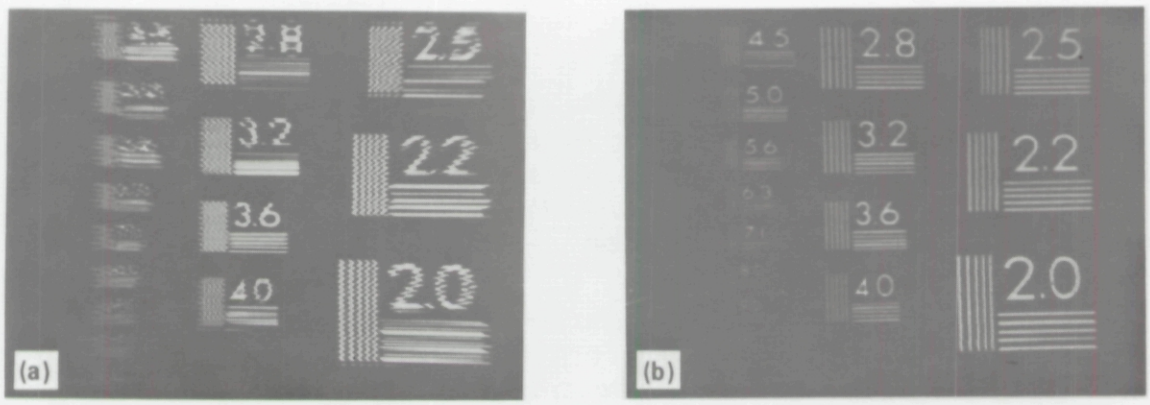

FIGURE 22. Images of navy resolution chart before (a) and after (b) "grounding" problems had been solved. The wiggles in image (a) are due to a 60 cycl-noise signal from unwanted ground loops when operating the TVI system at the end of the S.I.O. pier. See text for details.

The "natural environment" chosen for this series of tests turned out to be highly variable and to have very low values of transmittance. In Figure 23 the transmittance and tide level of the harbor water are plotted versus time during the period of our tests. The transmittance varied between 15%/meter ($1/\alpha = 0.53$ meters) and 1%/meter ($1/\alpha = 0.22$ meters) and significant changes were observed to take place over periods as short as several seconds. Note the alternate scale on Figure 23 showing that the attenuation length of the water during the four-hour period varied from roughly 1/2 to 1/4 meter water. The optical properties of such water severely limits conventional imaging systems and provided a severe test of the experimental TVI system.

A few color photographs taken at dusk during the harbor tests are shown in Figure 24. The white van, shown parked at the end of the S.I.O. pier in photograph (a), served as a field laboratory. It contained the control/storage/display unit (§II B2 and Figure 7) in addition to the transmissometer recorder and other equipments used during the tests. Photograph (b), taken from inside the van, shows the navy test chart used in these tests and the control/storage/display unit. Photographs (c) and (d) show the underwater unit about to be utilized by divers and give an indication of the low visibility (low transmittance) in the water. Even in daylight the divers would lose sight of each other if they were more than a few meters apart. At night fixed ropes and colored floats (seen in d) were attached to the underwater target and receiver so that the divers could relocate them when changes in experiment variables were made.

FIGURE 23. Transmittance [%/meter] and tide level [feet] versus time in San Diego Harbor at the end of the S.I.O. pier on 14 August 1974. A series of tests utilizing the experimental TVI system were performed during the period shown. The transmittance data has been replotted from a continuous recording which showed significant changes over periods as short as several seconds.

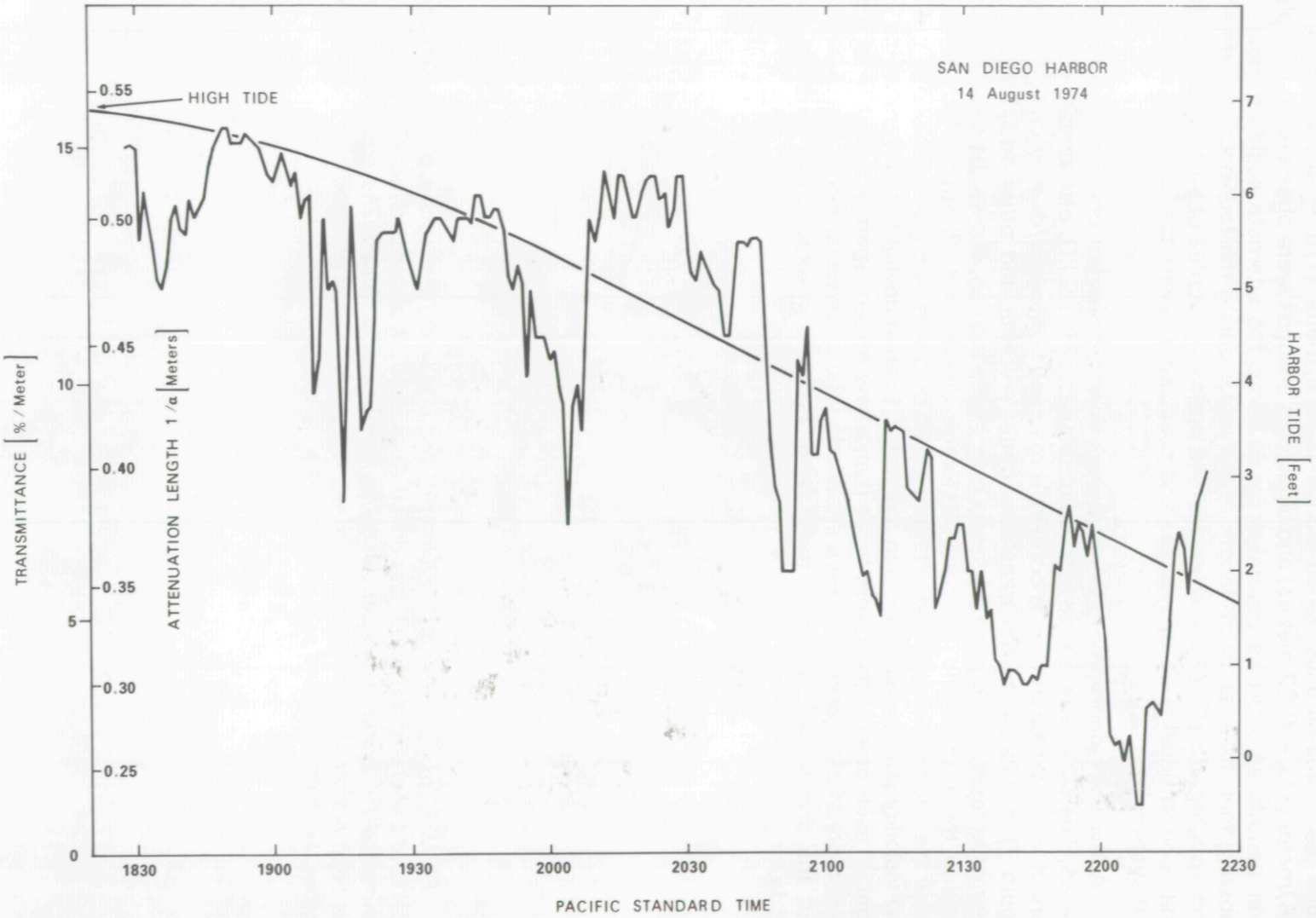
SAN DIEGO HARBOR
14 August 1974
HIGH TIME
0.55
0.50
0.45
0.40
0.35
0.30
0.25
15
10
5
0
TRANSMITTANCE [% / Meter]
ATTENUATION LENGTH 1 /α [Meters]
7
6
5
4
3
2
1
0
HARBOR TIDE [Feet]
1830
1900
1930
2000
2030
2100
2130
2200
2230
PACIFIC STANDARD TIME

(a)

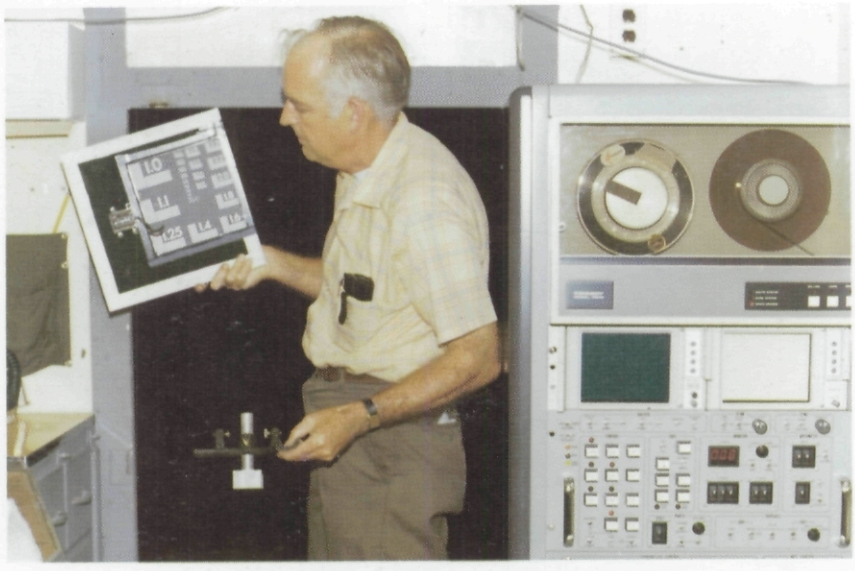

(b)

(c)

(d)

FIGURE 24. Photographs taken at dusk during the harbor tests. Photograph (a) shows the white van which was used as a field laboratory parked at the end of the S.I.O. pier. Photograph (b), taken from inside the van, shows the navy test chart and the TVI control/storage/display unit. Photograph (c), shows the underwater laser scanner being lowered to the divers. Photograph (d), shows a diver submerging with the underwater unit. Note that the underwater unit is almost lost from sight when only a meter or so below the surface, indicating water of very low visibility.

The experimental TVI system was used with the remote umbilical cable and also with battery power by a free-swimming diver. In order to maintain some control over the geometry of operation and to have quantitative knowledge of the operating distances, an underwater tripod and fixed ropes were used for the tests using the umbilical cable. This allowed us to obtain images in the harbor water while at the same time maintaining control over the distances r_1 and r_2. As a consequence we have quantitative knowledge of the experimental geometry for the harbor tests.

Figure 25 shows four images obtained using the experimental TVI system in San Diego Harbor. For this series of images the target-to-receiver distance, r_2, was held fixed while the laser scanner-to-target distance, r_1, was varied. These images show how the image contrast rapidly decreases and backscatter rapidly increases as r_1 is increased. The limit imposed by a maximum distance r_1 on image quality is analogous to the limiting distance in a conventional imaging system. Our tests indicate that the maximum value of r_1 is 3 to 4 attenuation lengths. Beyond this range light backscattered between the laser scanner and target reduces the image contrast to an unacceptable level. This backscattering is readily apparent in images (c) and (d). The "streaking" appearance of this backscattered light is presumably due to the larger scattering particles drifting between the target and the laser scanner while being repeatedly illuminated by the scanning laser beam.

Figure 26 shows a series of images obtained by holding r_1 fixed and varying r_2. These images show the decreasing image contrast as r_2 increases but also show that the numbers on the counter can be read even after the image has been propagated through nearly 24 attenuation lengths of water.

Data obtained from the images shown in Figure 26 were used to make a rough quantitative comparison with calculations using Equation A-11. Several adjacent white and black areas from the images in Figure 26 were used to estimate the relative white minus black signal in the images as recorded by the z-axis (intensity) monitor on the TVI display unit. These relative signal levels were obtained several days after the completion of the harbor tests by recalling the images from magnetic tape to the display monitor (§II C). By estimating the signal-to-noise ratio in image (d) the relative signal response for the remaining images can be calculated. The relative signal responses for these images is plotted in Figure 27 along with curves derived from Equation A-11 and the known parameters of the experimental TVI system. The average attenuation coefficient of the water when these images were propagated is known, but the relative scattering-to-absorption ratio is not. The relative signal response of the experimental TVI system has been plotted in Figure 27 with the scattering-to-absorption (s/a) ratio as a parameter.

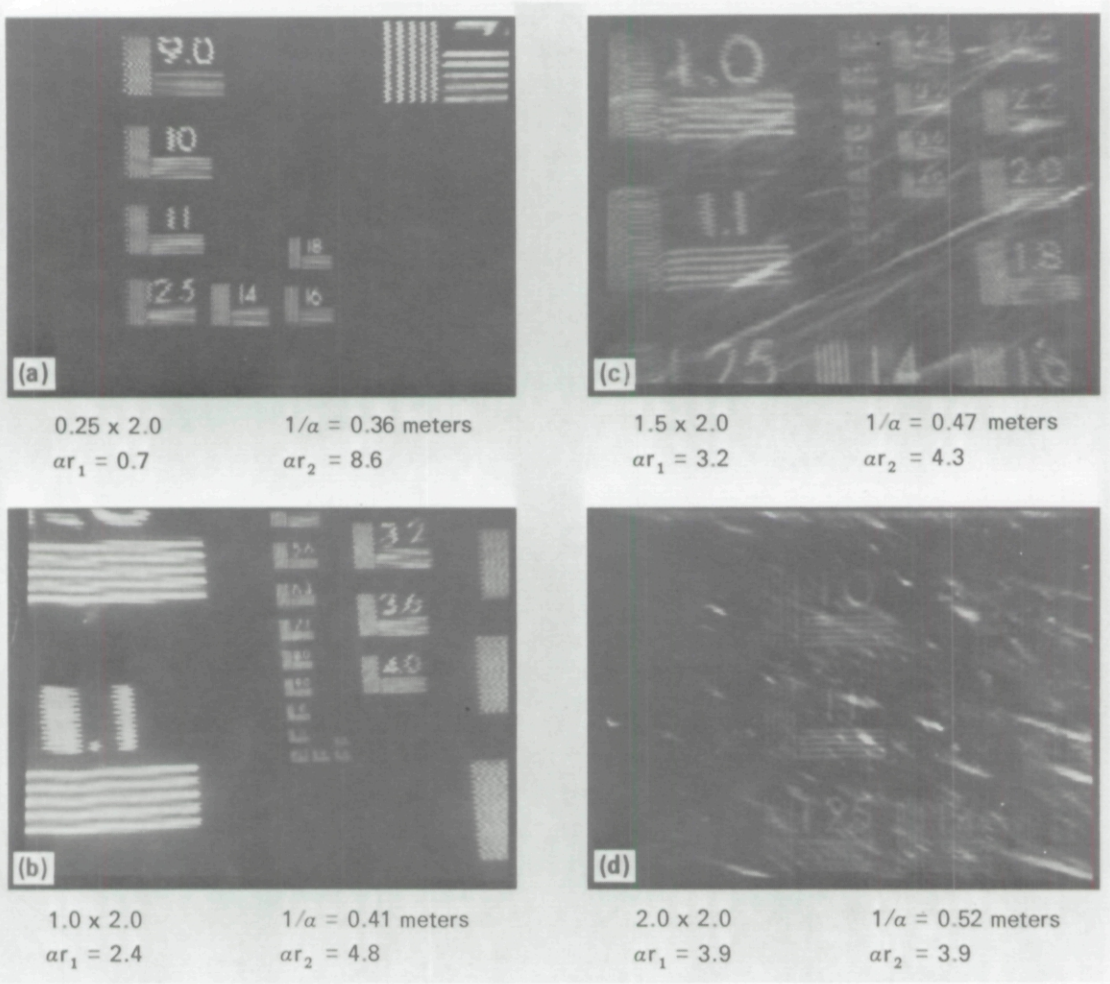

FIGURE 25. Images obtained using the experimental TVI system in San Diego Harbor. These images show the rapidly decreasing image contrast and increased image degradation due to backscattered light as the laser scanner-to-target distance is increased. The target-to-receiver distance, r_2, was held constant at 2.0 meters while the laser scanner-to-target distance, r_1, was varied from 0.25 to 2.0 meters. The attenuation length of the water varied from 0.52 to 0.36 meters during the time this set of images was obtained. The scan angle was held constant at $\sim 5^\circ$ for these images. The effect of extraneous noise, described with Figure 22, contributed to the degradation of these images.

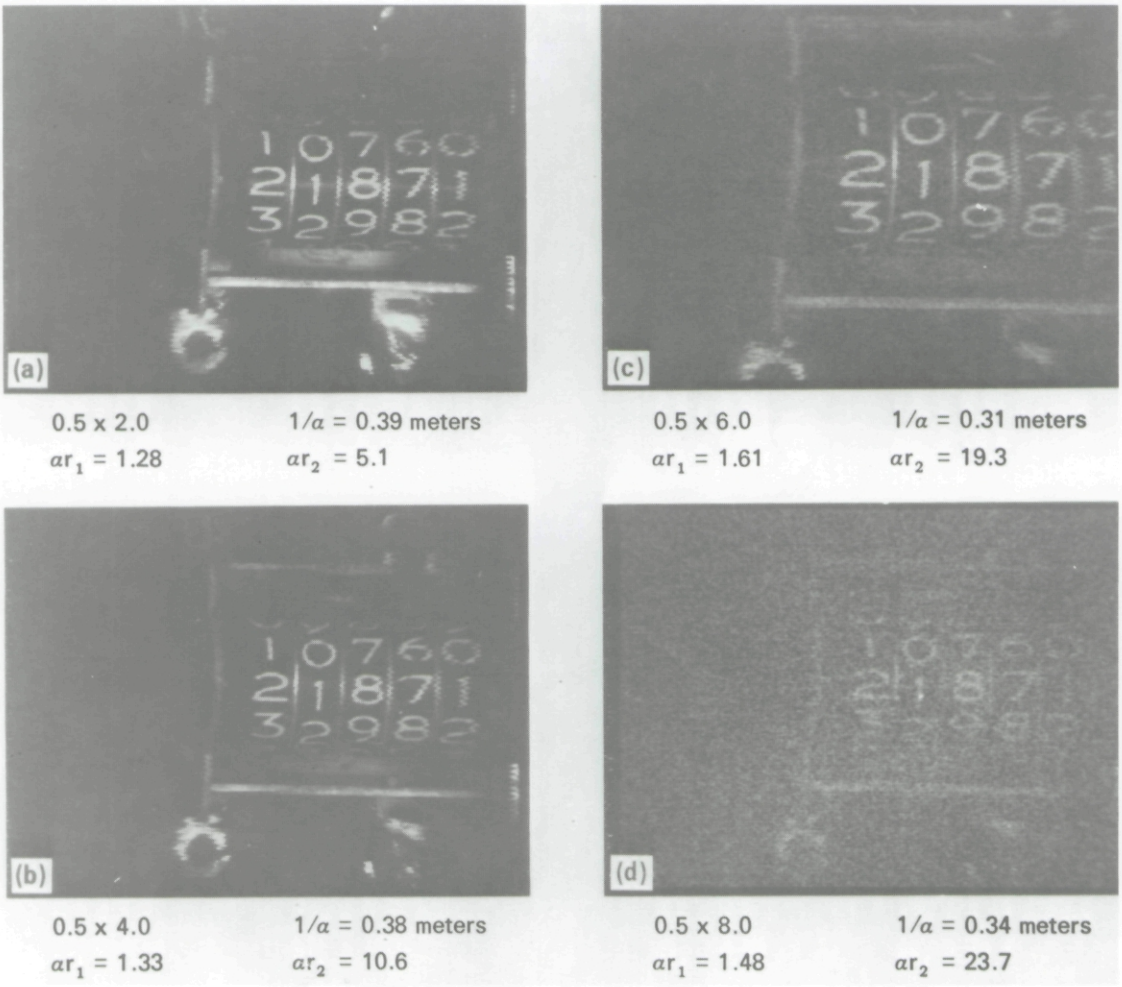

FIGURE 26. Images obtained using the experimental TVI system in San Diego Harbor. These images show the decreasing image contrast as the target-to-receiver distance is increased. In this series of images r_1 was held fixed and r_2 varied. The scan angle was constant at 5° for all images. Note that the numbers on the counter can be read even after the image has been propagated through nearly 24 attenuation lengths of very turbid water.

FIGURE 27. Graphs of relative signal response of the experimental TVI system vs. target-to-receiver distance using the scattering-to-absorption ratio (s/a) as a parameter. Solid curves were calculated from Equation A-11 (Part I) using the known parameters of the experimental TVI system and the measured optical properties of the water. Data shown as circles were derived from the relative white minus black intensity of selected areas in the images shown in Figure 26. See text for discussion.

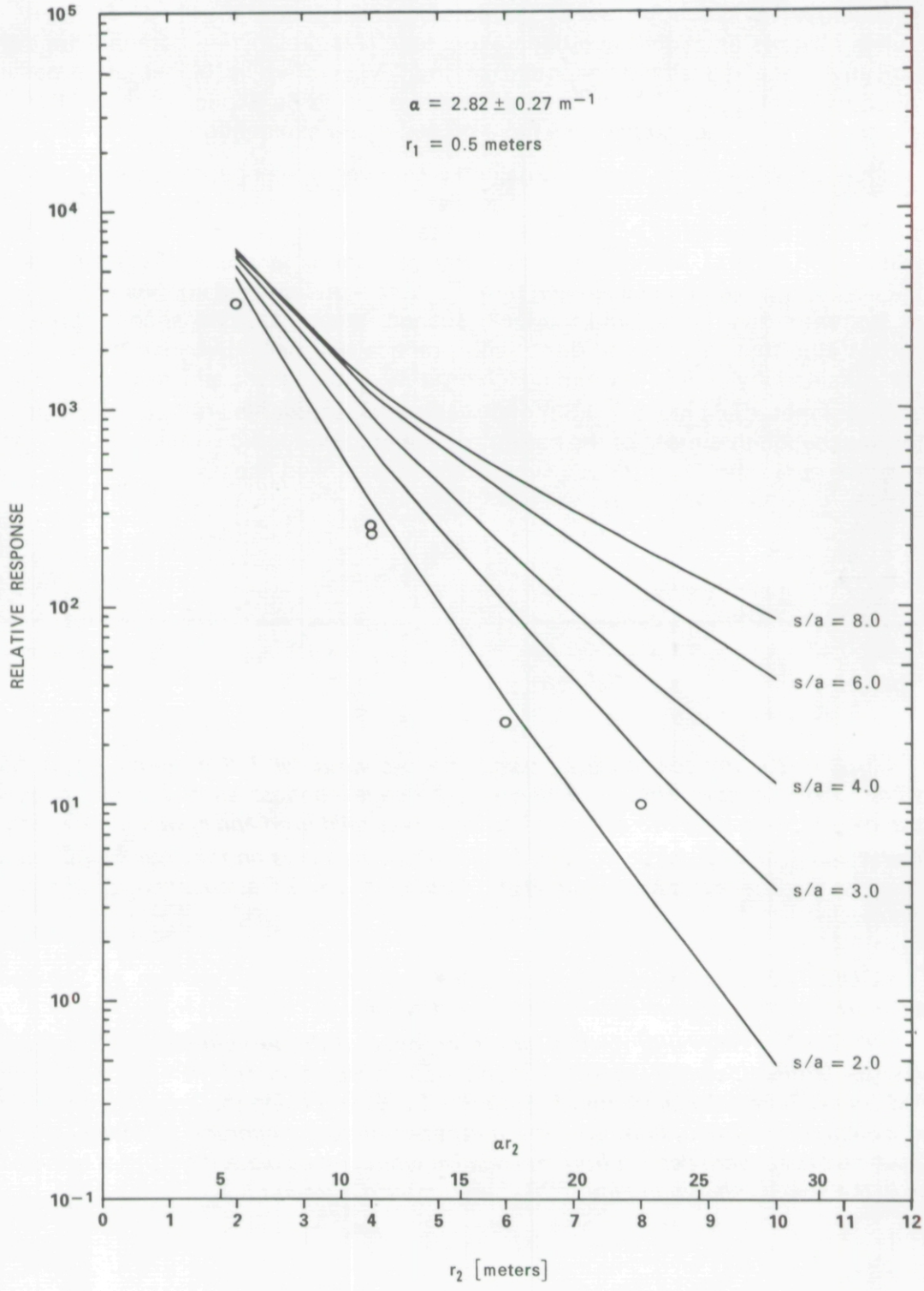
$\alpha = 2.82 \pm 0.27\ m^{-1}$
$r_1 = 0.5$ meters
RELATIVE RESPONSE
10^5
10^4
10^3
10^2
10^1
10^0
10^{-1}
s/a = 8.0
s/a = 6.0
s/a = 4.0
s/a = 3.0
s/a = 2.0
αr_2
5
10
15
20
25
30
0
1
2
3
4
5
6
7
8
9
10
11
12
r_2 [meters]

The absolute value of the data (circles on the graph) as compared to the values of the curves is as close as expected. The differences can be qualitatively explained by uncertainty in the value of the reflectance of the target and by the fact that losses in the receiver filter were not accounted for in Equation A-11. On the other hand the relative shape of the curve formed by the data does not follow the shape of any of the calculated curves as might have been expected. This preliminary data indicates that the relative received signal response of the TVI system is higher after passing through many attenuation lengths of water than would be expected on the basis of Equation A-11. At the moment we have no satisfying explanation for this result.

Figure 28 shows two images obtained by a diver while operating the experimental TVI system in San Diego Harbor. The distortion in image (a) is due to motion between the laser scanner (i.e., diver) and the target during the one-second scan time. As discussed in Part I, a limiting feature of the present experimental TVI laser scanner is the relatively slow image scanning rate. To obtain undistorted images with the present system a diver must hold the laser scanner steady for one second. Image (b) demonstrates that this can be done with practice and care. Because these images were obtained by a free-swimming diver, the distances r_1 and r_2 could only be roughly estimated. At night in 0.3 meter water such estimates are not very reliable. It is for this reason that most of the harbor tests were conducted with the laser scanner and target on a tripod and the receiver attached to a fixed line.

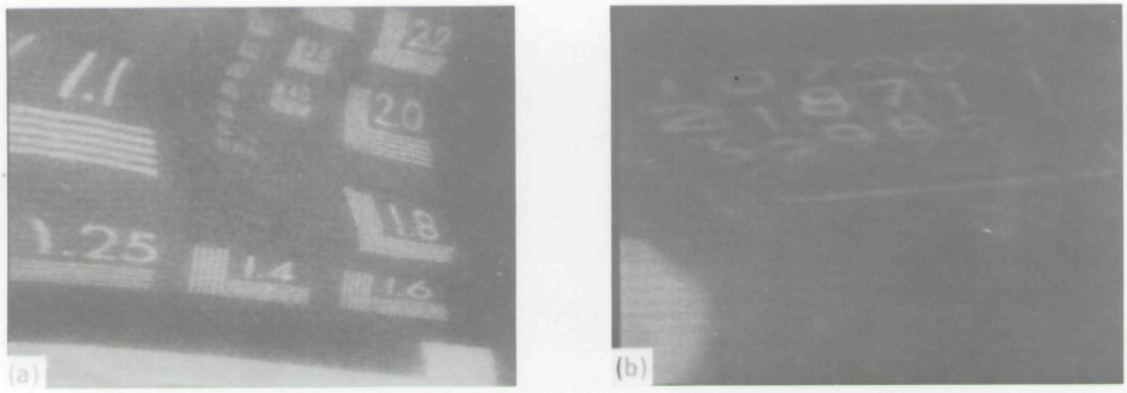

FIGURE 28. Images obtained using the experimental TVI system in San Diego Harbor. These images were obtained using battery power on the laser scanner by a free-swimming diver. The distortion in image (a) is due to motion between the laser scanner and target during the 1-second scan time (i.e., the diver was not holding the laser scanner steady). For these images the distances r_1 and r_2 have been roughly estimated to be 1/2 and 3 meters. The attenuation length of the water for images (a) and (b) were 0.29 and 0.35 meters respectively.

IV. SUMMARY

All of the specific objectives to be performed under Task 1 have been performed. These objectives were listed in the Work Statement of our contract proposal as follows:

"1. Design and fabricate a working model of a submersible laser scanner imaging system that will use scatter propagation from the illuminated scene to the receiver. The scanner will be battery operated and packaged in an underwater case not requiring any form of umbilical connection. Small lasers (40 milliwatts or less output) will be employed in the design. The scanner and its associated sweep and synchronization circuits will operate from the same battery power source."

Objective 1 has been fully completed, as described in Section II of this report. It should be noted that, in addition to the above requirements: the underwater housing for the laser scanner was built to be contained (exclusive of handles) within a 24 inch long by 12 inch diameter volume; the underwater laser scanner was equipped with supplementary controls in order to provide more quantitative engineering data while diver operated; and the underwater unit was built with the alternative possibility of using an umbilical cable for additional flexibility during testing and evaluation. Further, as discussed in detail in Section II, the design of the control/image storage/display unit went beyond providing the basic components and controls necessary for underwater operation by a diver by providing sufficient system flexibility to allow accurate quantitative data, along with each image, to be obtained for analysis of the TVI concept.

"2. The equipment described above will be tested in a laboratory-test tank to verify that it is performing in accordance with expectations."

The tests fulfilling objective 2 have been described in Section III B. As noted in Section III, the experimental TVI system performed beyond expectations. A continuation and extension of the effort described in this report will conduct additional laboratory tank measurements using the TVI system in order to quantitatively evaluate system performance in various waters.

"3. The equipment will be tested in nearby coastal waters. The primary objective of these tests will be to evaluate the feasibility of such a system in a semi-operational situation; i.e., using divers to operate the underwater equipment in harbor or ocean water with the image and synchronization information transmitted to the remote receiver by means of scattered light. During these tests, engineering data will be obtained on the signal, background and noise levels encountered. Water conditions at the time of the tests will also be documented. The images will be recorded directly by photography on the display monitor. Selected images will be digitized and recorded on magnetic tape."

The tests performed in San Diego Harbor have been described in Section III C. During the continuation and extension of the effort described in this report, a thorough engineering evaluation of this equipment will be performed in San Diego Harbor and in coastal waters in the San Diego area to obtain data on the dependence of system performance on environmental conditions.

"4. An evaluation will be made of all test results. Image quality determined both subjectively by viewing the photographs recorded during the tests and quantitatively by analysis of the images which have been digitally recorded. The image quality will be compared with the data recorded on signal, background, and noise levels as well as the data on water conditions at the time of the test to insure that the equipment is operating at its predicted level of performance. Image processing techniques will be applied if appropriate."

This report, especially the discussion of figures showing images obtained with the experimental TVI system, has described the fulfillment of this objective. Further efforts will aim at providing a phenomenological theory so as to quantitatively describe TVI system performance.

5. Objective 5, not directly related to the construction and testing of the experimental TVI system, has been discussed in a separate memorandum.